ORGANOMETALLICS

Article

pubs.acs.org/Organometallics

Synthesis and Structure of Group 4 Symmetric Amidinate Complexes and Their Reactivity in the Polymerization of α-Olefins

Tatyana Elkin,[†] Naveen V. Kulkarni,[†] Boris Tumanskii,[†] Mark Botoshansky,[†,§] Linda J. W. Shimon,[‡] and Moris S. Eisen*[,†]

[†]Schulich Faculty of Chemistry, Technion−Israel Institute of Technology, Haifa 32000, Israel

[‡]Department of Chemical Research Support, Weizmann Institute of Science, Rehovot 76100, Israel

Supporting Information

ABSTRACT: The steric properties of various nitrogen substituents on amidines were tuned in order to obtain group 4 mono- and bis(amidinate) dimethylamido or chloride complexes. The amidinate dimethylamido and chloride complexes were prepared, and their solid-state as well as their solution-state structures were studied. After the activation by MAO, these complexes were tested in the polymerization of propylene and ethylene. A noticeable influence of the amidine carbon and nitrogen substituents on the activity of the catalyst and properties of the obtained polymer was observed. Further, a plausible mechanism for the ethylene polymerization process is presented taking into account a combination of ESR-C_{60} and MALDI-TOF experiments, shedding light on the nature of the catalytic species.

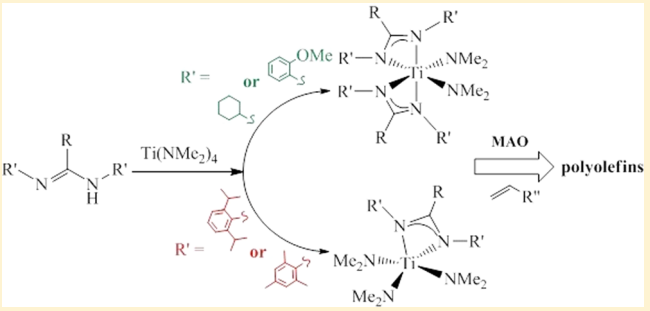

INTRODUCTION

The design and synthesis of the well-defined homogeneous catalysts for the polymerization of α-olefins remains an area of immense interest in academic as well as industrial applications.[1−3] A large number of catalysts developed in this area of research are metallocenes[1c−f,2g−j,4−7] and half-metallocenes;[2b,e,f,j,8−11] however, an extensive number of post-metallocene complexes containing chelating ancillary ligands have received considerable attention in recent years.[2e,f,k,m,n,9b,12−15]

The amidinate ligands are considered to be sterically equivalent to the cyclopentadienyl ligands, varying most significantly in their electronic properties.[8h,9a,10d] The amidinate group $[R^1\text{-}C(NR^2)_2]^-$ is a four-electron donor, as compared to the six electrons of the cyclopentadienyl ligand, in turn offering a higher electrophilicity at the metal center in such complexes.[13a−d,14a,b,15b,16] Amidinate ligands are particularly attractive owing to the ease with which they may be modified, producing ligands with specific steric and electronic constraints. The combination of these factors as well as the facile synthetic protocols for this class of ligands has allowed for the production of various organometallic complexes useful for the polymerization of α-olefins.[13−15]

Previous research in our group has revealed that group 4 bis(benzamidinate) dichloride and dialkyl complexes, when activated by methylaluminoxane (MAO), form catalytically active species, which can polymerize propylene, affording a mixture of isotactic and elastomeric polypropylenes.[17] The mechanistic studies have suggested that the activation of the complexes takes place via two pathways. The first route involves the formation of a cationic bis-amidinate alkyl complex as the active species and yields an isotactic fraction. The second route involves the formation of a cationic monoamidinate dialkyl complex, resulting from ligand dissociation of the bis-(amidinate) complex and its migration to an aluminum moiety in MAO; the resulting mono(benzamidinate) entity produces the elastomeric polypropylene due to the open coordination site.[14b,17]

In addition, we have demonstrated that after the mono-(benzamidinate) species are formed, the remaining amidinate ligand may undergo a rearrangement, producing a κ^6 coordination through the *ipso*-phenyl substituent, inducing steric hindrance between the *para*-substituent of the ring and the growing polymer chain. This interaction will prevent the polymeric chain termination and correspondingly aid the formation of polymers with higher molecular weights. Changing the substituents at the *para*-position of the aryl group revealed that bulkier substituents lead to the formation of polymers with higher molecular weights and correlates with a linear free energy relationship of the *para*-substituent with the Taft steric parameter (Scheme 1).[18]

Group 4 complexes containing amidinate ligands with an isopropyl substituent at the *ipso*-position, instead of an aryl group, do not form stereospecific polypropylenes when activated by MAO. This is due to the dynamic behavior of the complexes, which leads to the complete loss of the C_2-symmetry around the metal center. Interestingly, introduction of fluorine atoms into different positions of an amidinate N-

Received: July 16, 2013

   dx.doi.org/10.1021/om4006998 | *Organometallics* XXXX, XXX, XXX−XXX

Scheme 1. Plausible Mechanism for the Formation of a Mixture of Isotactic and Elastomeric Polypropylene by Titanium Bis(amidinate) Complexes

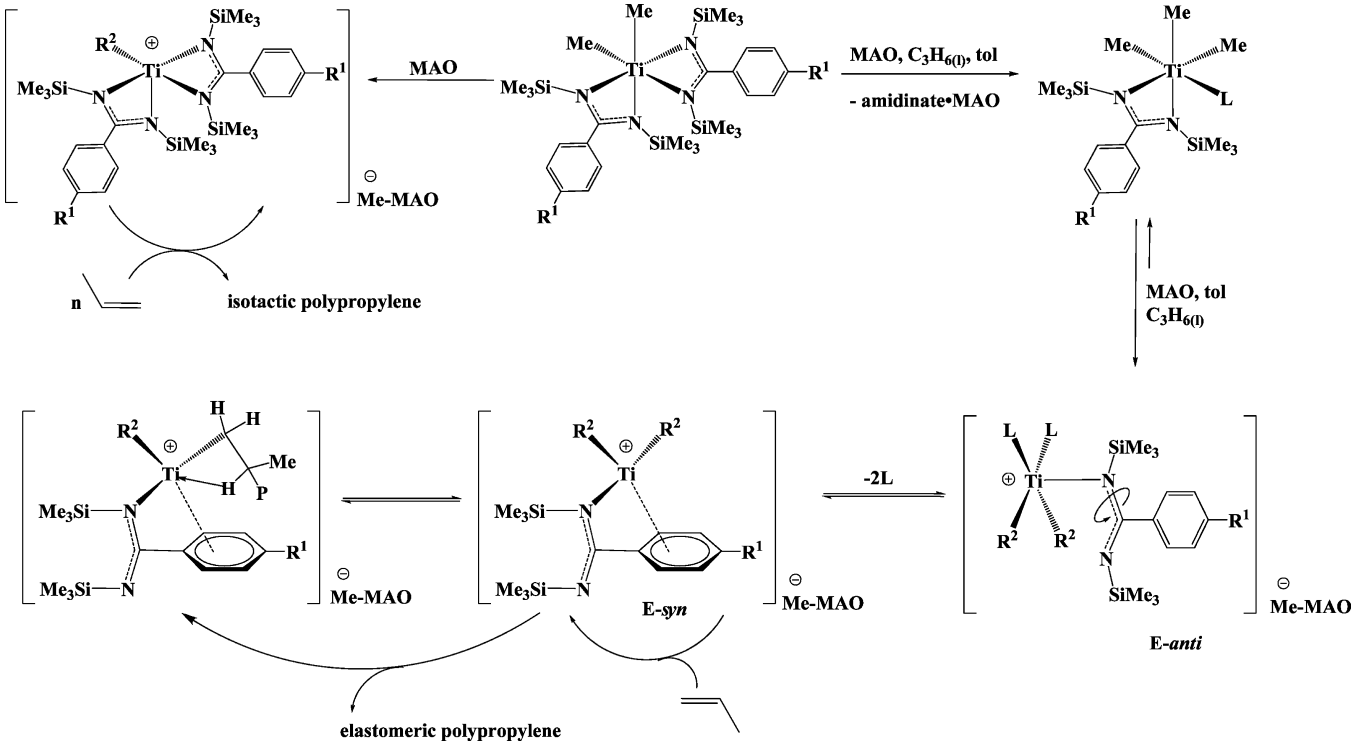

phenyl substituent revealed that the *meta*-fluorinated ligand aids in the suppression of the rate of termination of the growing chain, whereas a *para*-fluorine accelerates the rate of insertion of the monomer.[18]

The research presented in this work investigates the effect of electron-donating functionalities at the amidinate nitrogen. Furthermore, we were interested in studying the effect of an additional chelating site containing an electron-donating group in the *ortho*-position of the N-aryl substituent. In order to avoid the κ^6 coordination through the *ipso*-phenyl substituent, the *ipso*-position of the amidinate ligand has been substituted with hydrogen, methyl, or ethyl moieties. Herein we report the synthesis of various titanium and hafnium amidinate complexes, their crystallographic structures, and their catalytic performance in the polymerization of ethylene and propylene. We present a combination of ESR, C_{60} radical trapping, and MALDI-TOF studies describing the formation of the active species, trapping some unique features of the complexes and shedding light on the polymerization mechanism.

RESULTS AND DISCUSSION

Synthesis and Structure of Ligands. As has been previously demonstrated, the presence of the fluorine atoms on the N-phenyl rings reduces the electron density over the amidinate HN-C═N backbone and induces dissociation and rearrangement of the ligand about the metal center.[19] We expect that placing electron-donating groups should increase the electron density over the coordination cavity, increasing the ligand-to-metal bond strength, and further inhibiting ligand migration. Furthermore, the introduction of additional coordinating groups to the ligand structure potentially increases the denticity of the resulting ligand in the metal complex. In consideration of these factors, a series of amidinate ligands have been prepared, which incorporate 2,6-diisopropylphenyl, mesityl, cyclohexyl, and *o*-methoxyphenyl groups as the amidinate N-substituents. In order to minimize possible steric effects or π bonding of the *ipso*-carbon substituent, this position has been occupied by proton, methyl, or ethyl moieties.

The corresponding alkyl amidines were prepared in high yields following literature procedures by heating the suitable amine with the respective *ortho*-esters in a 2:1 ratio, in the presence of catalytic amounts of HCl or AcOH (eq 1).[20] Ligand

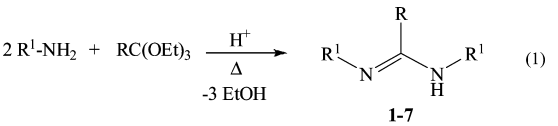

1-7

1 R^1 = 2,6-diisopropylphenyl; R = H
2 R^1 = mesityl; R = H
3 R^1 = mesityl; R = Me
4 R^1 = cyclohexyl; R = H
5 R^1 = *o*-anisyl; R = H
6 R^1 = *o*-anisyl; R = Me
7 R^1 = *o*-anisyl; R = Et

7 has not been reported in the literature and was obtained in 92% yield. Ligand **7** was crystallized from an ethanol/water (70:30) solution, and its solid-state structure is presented in Figure 1. (The crystal data and refinement details for ligand **7** are presented in the Supporting Information.)

In the solid state, ligands **6** (Supporting Information) and **7** are isostructural, indicating that the *ipso*-C substitution does not affect the amidine motif.[21] In both ligands, one of the phenyl rings is disposed in the same plane as that of the amidine N═C-NH backbone, whereas the other is situated nearly orthogonal (torsion angles, 92.52° and 87.74° for ligands **6** and **7**, respectively). Although the groups at the *ipso*-carbon are

dx.doi.org/10.1021/om4006998 | *Organometallics* XXXX, XXX, XXX–XXX

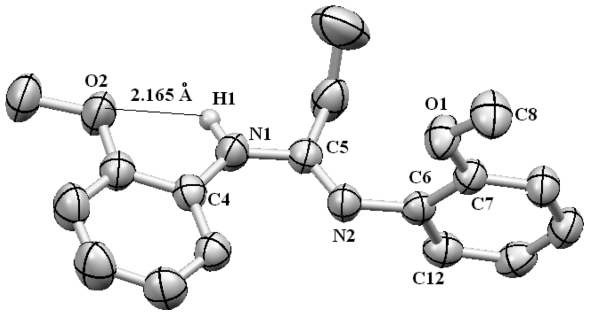

Figure 1. Mercury presentation of the molecular structure of ligand **7** showing the hydrogen bond interaction between the OMe moiety and the N−H amidine group (50% probability ellipsoids). Hydrogen atoms (besides the amidine N−H) were removed for clarity. Representative bond lengths (Å) and angles (deg): C(5)−N(1) = 1.3743(16); C(5)−N(2) = 1.2731(16); C(4)−N(1) = 1.4023(17); C(6)−N(2) = 1.4099(16); C(7)−O(1) = 1.3681(16); C(8)−O(1) = 1.4206(18) Å; N(2)−C(5)−N(1) =120.66(12); C(7)−O(1)−C(8) = 117.70(11); C(5)−N(2)−C(6)−C(12) = 87.74°.

small, it seems that they are sterically bulky enough to force one of the N-phenyl rings to an *anti*-position, leading to a *trans-syn* tautomeric form (**III** in Scheme 2). The OMe group at the *ortho*-position forms a hydrogen bond with the amidine N−H due to the favorable distance for a typical intramolecular hydrogen bond[22] (2.176 and 2.164 Å for ligands **6** and **7**, respectively) and brings the corresponding phenyl ring and the amidine backbone into the same plane, serving to stabilize the resulting structure. Interestingly, in a similar system when the substituent at the *ipso*-carbon position is a hydrogen (ligand **5**), both phenyl rings are coplanar with the amidine moiety.[23]

Häfelinger and Kuske[24] have defined the parameter Δ_{CN} = d(C−N) − d(C═N) (where d is the bond length in Å) for the central N−C−N linkage of amidines. This parameter ranges from 0 (in a *trans-anti* hydrogen-bonded dimer (**V** in Scheme 2)) to 0.178 Å (in an amidine where conjugation is minimized due to bulky substituents on both nitrogen and carbon atoms). In our case, the parameter Δ_{CN} values are found to be 0.113 and 0.101 Å for ligands **6** and **7**, respectively, corroborating a localization of the proton on a particular nitrogen atom due to the strong intramolecular hydrogen bonding between the *o*-OMe group and the amidine N−H group.[24]

In solution, the amidine ligands generally exhibit various tautomeric structures, making the NMR studies complex for the study of these forms (Scheme 2).[25,26] ^{1}H NMR solution studies of ligand **7** show as expected two different methoxy groups at room temperature corroborating with the solid-state structure.

Synthesis and Structure of Mono(amidinate) Complexes. In the preparation of the Ti complexes **8**−**14**, $Ti(NMe_2)_4$ was used as a metal precursor. The titanium complexes bearing amidinate ligands with different steric bulk were chosen to investigate the steric effect on their coordination behavior. We have found that when one equivalent of $Ti(NMe_2)_4$ was treated with either one, two, or three equivalents of ligand **1**, the pentacoordinative mono(amidinate) tri(dimethylamido) complex **8** was always obtained (eq 2). Heating in toluene and/or increasing the reaction time

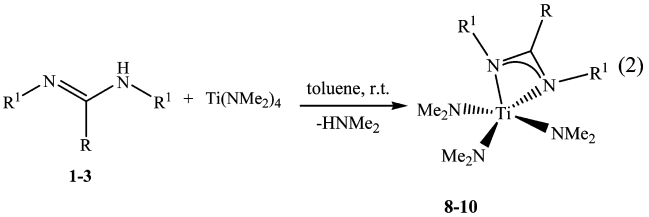

(2)

8 R = H; R^1 = 2,6-diisopropylphenyl
9 R = H; R^1 = mesityl
10 R = Me; R^1 = mesityl

did not yield any other product. Single crystals of complex **8** were obtained by slow evaporation of a hexane solution, and the solid-state structure is presented in Figure 2. (The crystal data and refinement details for complex **8** are provided in the Supporting Information.)

The mono(amidinate) complex **8** (Figure 2) exhibits a five-coordinative geometry and is best described as three-legged piano stool where the amidinate moiety is at the apical (bench) position.[27] From the crystal structure it is evident that once the

Scheme 2. Plausible Tautomeric Structures for Amidines in Solution

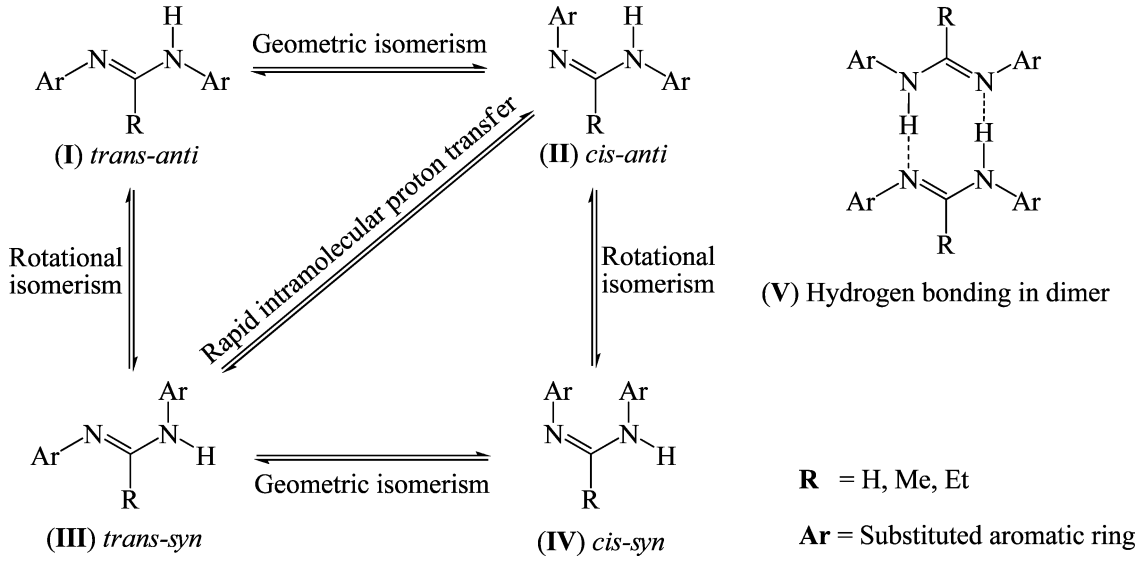

dx.doi.org/10.1021/om4006998 | Organometallics XXXX, XXX, XXX−XXX

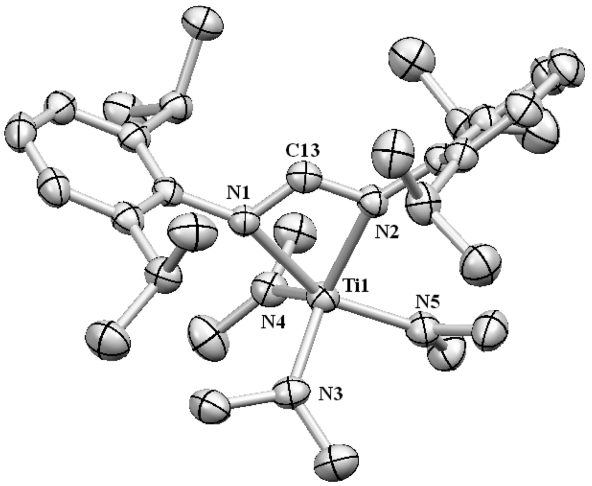

Figure 2. Mercury presentation of the molecular structure of complex **8** (50% probability ellipsoids). Hydrogen atoms are omitted for clarity. Representative bond lengths (Å) and angles (deg): Ti(1)−N(1) = 2.2926(13); Ti(1)−N(2) = 2.1847(13); Ti(1)−N(3) = 1.9087 (15); Ti(1)−N(4) = 1.9002(14); Ti(1)−N(5) = 1.9130(14); C(13)−N(1) = 1.310(2); C(13)−N(2) = 1.328(2) Å; N(2)−Ti(1)−N(1) = 60.20(5); N(2)−Ti(1)−N(3) = 123.28(6); N(3)−Ti(1)−N(5) = 98.64(6); N(4)−Ti(1)−N(3) = 106.77(6); N(1)−C(13)−N(2) = 116.87(15); N(2)−Ti(1)−N(1)−C(13) = 3.69°.

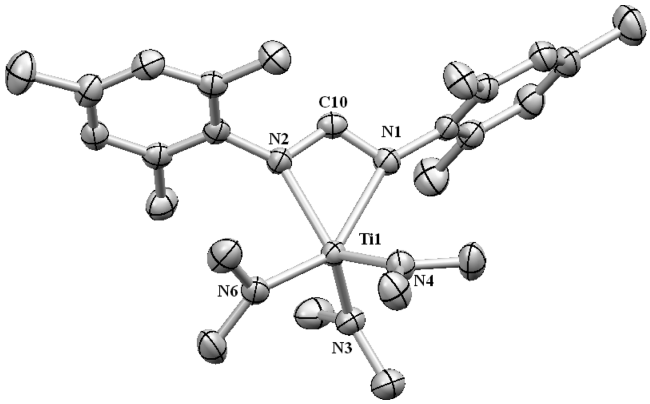

Figure 3. Mercury presentation of the molecular structure of complex **9** (50% probability ellipsoids). Hydrogen atoms are omitted for clarity. Representative bond lengths (Å) and angles (deg): Ti(1)−N(1) = 2.3087(12); Ti(1)−N(2) = 2.1372(12); Ti(1)−N(3) = 1.8838(13); Ti(1)−N(4) = 1.9115(13); T(1)−N(5) = 1.9197(13); C(10)−N(1) = 1.3055(19); C(10)−N(2) = 1.3251(19) Å; N(2)−Ti(1)−N(1) = 59.56(4); N(2)−Ti(1)−N(5) = 89.51(5); N(2)−Ti(1)−N(4) = 124.29(5); N(1)−C(10)−N(2) = 114.55(13); N(2)−Ti(1)−N(1)−C(13) = 5.74°.

first ligand has been coordinated to the metal center, due to its large cone angle (208°), an additional amidinate ligand will not be able to insert, hence yielding specifically the corresponding mono(amidinate) complex.

Decreasing the steric bulk of the ligands from the diisopropylphenyl motif (ligand **1**) to the slightly less sterically demanding mesityl substituents (ligands **2** and **3**) did not allow the insertion of a second coordinating ligand, also producing always the corresponding monoamidinate complexes, **9** and **10**, respectively (eq 2), regardless of the amount of the ligands and the reaction conditions.

The X-ray diffraction studies performed in single crystals of complexes **9** (Figure 3) and **10** (Figure 4) show also pentacoordinative complexes like that observed in complex **8**. (The crystal data and refinement details for complexes **9** and **10** are presented in the Supporting Information.)

From the crystal structures we can learn that ligands **2** and **3** are still bulky enough, inducing large cone angles at the metal center (complex **9** = 181°; complex **10** = 184°), preventing the insertion of a second ligand, thereby producing only the corresponding monoamidinate complexes.

Interestingly, in all three mono(amidinate) titanium complexes (**8**−**10**), the M−N bond lengths of the coordinated amidinates are nonsymmetric (complex **8**: Ti(1)−N(1) = 2.2926(13); Ti(1)−N(2) = 2.1847(13) Å, complex **9**: Ti(1)−N(1) = 2.3087(12); Ti(1)−N(2) = 2.1372(12) Å, and complex **10**: Ti(1)−N(1) = 2.181(4); Ti(1)−N(2) = 2.232(4) Å), due to the different dispositions of the amidinate nitrogen relative to the amido groups. One nitrogen atom of the amidinate ligand is almost located *trans* (∼150−160°) to one of the three amido groups, whereas the second amidinate nitrogen is situated between two amido groups (∼120−130°). Small torsion angles of the amidinate ligand in complexes **8**, **9**, and **10** (N(2)−Ti(1)−N(1)−C(13) = 3.69°, N(2)−Ti(1)−N(1)-C(13) = 5.74°, and N(2)−Ti(1)−N(1)−C(10) = 0.2(2)°,

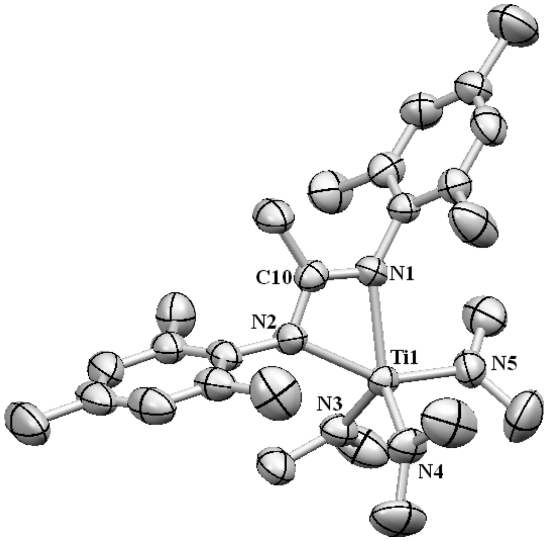

Figure 4. Mercury presentation of the molecular structure of complex **10** (50% probability ellipsoids). Hydrogen atoms are omitted for clarity. Representative bond lengths (Å) and angles (deg): Ti(1)−N(1) = 2.181(4); Ti(1)−N(2) = 2.232(4); T(1)−N(3) = 1.904(4); Ti(1)−N(4) = 1.901(4); Ti(1)−N(5) = 1.939(4); C(10)−N(1) = 1.327(6); C(10)−N(2) = 1.317(6) Å; N(2)−Ti(1)−N(1) = 59.92(14); N(1)−Ti(1)−N(5) = 91.63(16); N(5)−Ti(1)−N(4) = 99.73(19); N(1)−Ti(1)−N(4) = 128.07(16); N(1)−C(10)−N(2) = 113.0(4); N(2)−Ti(1)−N(1)−C(10) = 0.2(2)°.

respectively) indicate that the ancillary ligand is connected in a σ-fashion.

The Ti−N bond lengths of the mono(amidinate) complexes **8** and **9** are found to be longer as compared to all other reported amidinate complexes. According to the literature, most of the Ti−N (amidine) bond lengths (>95%) fall in the range 2.030−2.275 Å[28] with the longest bond reported as 2.312(4) Å in a silyl-linked bis(amidinate)-cyclopentadienyl mixed complex.[29] The monoamidinate complexes **8** and **9** presented here are the third and second longest Ti−N bonds reported for chelating amidinate complexes, respectively.

dx.doi.org/10.1021/om4006998 | *Organometallics* XXXX, XXX, XXX−XXX

Interestingly, in complex **10**, the Ti−N (amidine) bond lengths fall within the literature reported range. It seems plausible that the methyl group at the *ipso*-carbon of the amidinate moiety in complex **10** donates electron density into the amidinate moiety, resulting in stronger metal−nitrogen bonds as compared to a hydrogen atom in a similar position in complex **9**.

Synthesis of Bis(amidinate) Complexes. When two equivalents of ligand **4**, which bears a cyclohexyl group on the amidinate nitrogens, was reacted with $Ti(NMe_2)_4$ in toluene, the corresponding bis(amidinate) complex **11** (eq 3) was obtained in high yield. This result indicates that the cyclohexyl groups are flexible enough to allow the formation of bis(amidinate) complexes.[30]

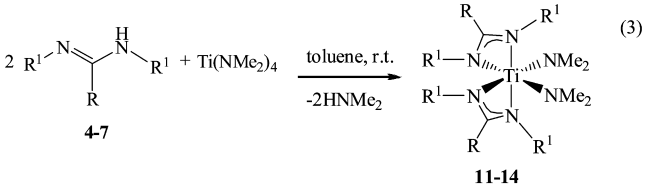

(3)

11 R = H; R^1 = cyclohexyl
12 R = H; R^1 = *o*-anisyl
13 R = Me; R^1 = *o*-anisyl
14 R = Et; R^1 = *o*-anisyl

The *ortho*-methoxy motif (ligands **5**, **6**, and **7**) is considered to be less bulky as compared to the diisopropyl and mesityl substituent groups[31] and may be used in order to prepare the corresponding bis(amidinate) complexes having an additional chelation and an electron-donating group.

The reaction of ligand **5** with $Ti(NMe_2)_4$ in a 2:1 ratio exhibits a very peculiar behavior. At room temperature in toluene, the corresponding bis(amidinate) complex **12** was obtained when the product was isolated within the first two hours (eq 3), while if the reaction mixture was stirred for additional periods of time (beyond this two hours), an insoluble deep dark red precipitate was obtained. When the same reaction was performed in hexane, the corresponding complex **12** could be isolated within the first four hours; however leaving the reaction mixture for longer periods of time resulted in the formation of the same precipitate. When the reaction was carried out in THF, the isolation of the complex **12** was achieved only in the first hour of the reaction. Interestingly, when analytically pure complex **12** was allowed to stand in a toluene solution overnight (15 mg/mL), the formation of the same dark red precipitate was observed; it is likely that the resulting precipitate is polymeric in nature due to its insolubility in various polar solvents. These results indicate that complex **12** is probably a kinetic product of the reaction, whereas the precipitate seems to be the thermodynamic one. On the other hand, the reaction of ligands **6** and **7** with $Ti(NMe_2)_4$ in a 2:1 ratio yields only the expected monomeric bis(amidinate) complexes **13** and **14**, respectively, in high yields, regardless of the reaction conditions (eq 3). Interestingly, the different behavior of complex **12**, as compared to **13** and **14**, relates to the substitution at the *ipso*-carbon of the amidinate moiety. In complex **12**, the presence of the amidinate hydrogen, which is acidic (appearing in the ^{1}H NMR at δ = 9.36 ppm in the complex, as compared to δ = 8.25 ppm in the free ligand), presumably forms a hydrogen bond with a methoxide group, producing the observed polymeric material. It is important to point out that in complexes **13** and **14** the steric interaction of the *ipso*-carbon substituents restricts the rotation of N-phenyl rings (based on the X-ray of complex **14**), thus preventing the interaction of the *o*-methoxy groups with other metal centers.

The solid-state structure of the titanium bis(amidinate) complex **14** (Figure 5) exhibits a pseudo-octahedral geometry.

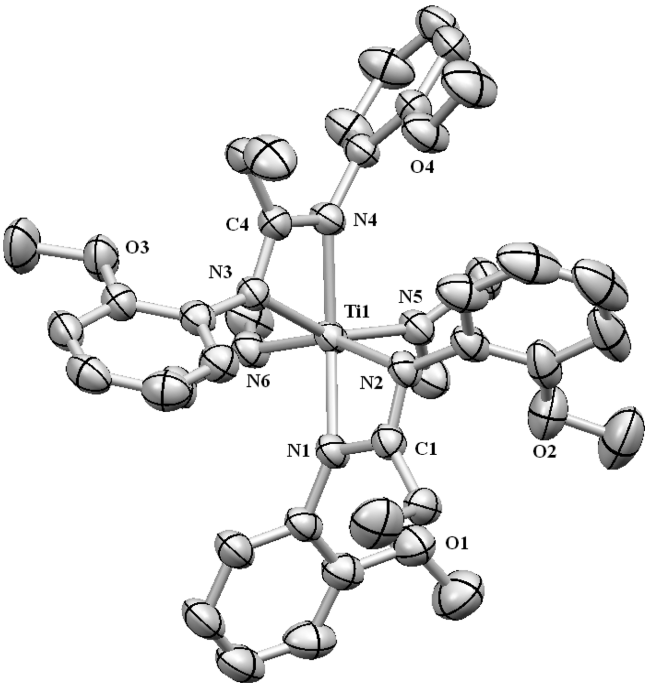

Figure 5. Mercury presentation of the molecular structure of complex **14** (50% probability ellipsoids). Hydrogen atoms are omitted for clarity. Representative bond lengths (Å) and angles (deg): Ti(1)−N(1) = 2.103(3); Ti(1)−N(2) = 2.221(3); Ti(1)−N(3) = 2.186(3); Ti(1)−N(4) = 2.107(3); Ti(1)−N(5) = 1.883(3); Ti(1)−N(6) = 1.901(3); C(1)−N(1) = 1.343(4); C(1)−N(2) = 1.311(4) Å; N(2)−Ti(1)−N(1) = 60.49(10); N(5)−Ti(1)−N(2) = 91.82(12); N(2)−Ti(1)−N(1)−C(1) = 5.54; N(4)−Ti(1)−N(3)−C(4) = 0.03.

(The crystal data and refinement details for complex **14** are presented in the Supporting Information.) The dimethylamido groups are disposed in a *cis*-position, N(5)−Ti(1)−N(6) = 100.48(13)°, providing a pseudo-C_2-symmetry for the complex. Each dimethylamido group is disposed opposite one of the amidinate nitrogen atoms. The Ti−N bond lengths of the dimethylamido groups (1.883(3) and 1.901(3) Å) and the Ti−N bond lengths of the coordinated amidinate ligands (2.103(3), 2.221(3), 2.107(3), and 2.186(3) Å) are comparable to previously reported amidinate complexes.[18,19] Both of the amidinate ligands are connected in a σ-fashion (torsion angles N(2)−Ti(1)−N(1)−C(1) = 5.54°; N(4)−Ti(1)−N(3)−C(4) = 0.03°).

The observed asymmetry of the amidine N−Ti bond lengths are due to the *trans* influence of the corresponding amido moieties (angles, N(6)−Ti(1)−N(2) = 156.22(11)°, N(5)−Ti(1)−N(3) = 152.26(11)°).[18]

It is important to note that our attempts to prepare mono(amidinate) complexes with ligands **5**, **6**, and **7**, under various conditions, were unsuccessful. In all cases the bis(amidinate) complexes were always obtained (complex **12**

dx.doi.org/10.1021/om4006998 | *Organometallics* XXXX, XXX, XXX−XXX

forms and then precipitates as described above). Interestingly, when each of the ligands **5**, **6**, and **7** were reacted with each of the mono(amidinate) complexes **8**, **9**, and **10**, under various conditions, the corresponding bis(amidinate) complexes **12**, **13**, and **14**, respectively, were obtained; however no mixed ligand bis(amidinate) complexes were obtained. This is likely due to the strong coordination of ligands **5**, **6**, and **7** to the metal center, displacing the former ligands. This result indicates that the *o*-methoxide-containing amidinate ligands are more nucleophilic than the amidinate ligands containing the mesityl and diisopropylphenyl moieties.

In order to obtain the corresponding dichloride complexes, the lithium salts of the ligands were produced by the reaction of the neutral ligands with ^{n}BuLi, followed by the reaction with $TiCl_4$·2THF. When ligand **5** was treated with ^{n}BuLi, in toluene or THF, an insoluble lithium complex was formed. Our attempts to react this precipitate, *in situ*, with the metal precursor under the various reaction conditions were not successful in obtaining the desired bis(amidinate) dichloride complex and resulted in the formation of a myriad of products. The lithium salts of ligands **6** and **7** were easily prepared *in situ* (followed by ^{1}H NMR) to obtain the corresponding complexes **6a** and **7a** (eq 4). When two equivalents of the lithium salts **6a**

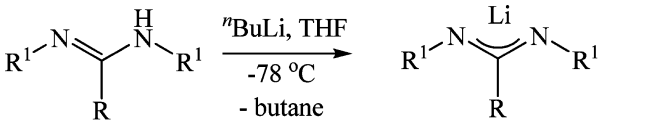

6, 7

6a R = Me, R^1 = *o*-anisyl
7a R = Et, R^1 = *o*-anisyl

(4)

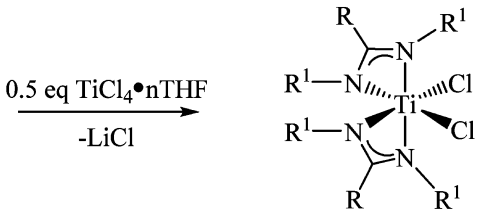

15, 16

15 R = Me; R^1 = *o*-anisyl
16 R = Et; R^1 = *o*-anisyl

and **7a** were reacted with one equivalent of $TiCl_4$·2THF, the bis(amidinate) dichloride complexes **15** and **16** were obtained, respectively (eq 4). Interestingly, when we tried to synthesize the corresponding zirconium complexes by reacting the lithium salts of the ligands (**6a** or **6b**) with $ZrCl_4$·2THF, we were unable isolate the desired bis(amidinate) complex. When the same reaction was performed between three or one equivalent of the ligand **6a** and $HfCl_4$, either the corresponding tris- or the mono(amidinate) complex was obtained (complex **17** and **18**, respectively) (Scheme 3). However the latter complex was always obtained with some amount of the corresponding tris(amidinate) complex (~10%). This result indicates that the energy of activation to replace the second chloride of the metal precursor after the first metathesis of the ligand must be higher than that of the corresponding third chloride.

All the bis(amidinate) complexes in this study show fluxional behavior in solution at room temperature. This fluxionality may involve various processes including opening ($\kappa^2 \rightarrow \kappa^1$) and closing ($\kappa^1 \rightarrow \kappa^2$) of the amidinate ligand,[19] a Bailar rotation,[30] or a methoxide interaction with the metal center. In the case of complex **14**, the thermodynamic parameters ($\Delta H^{\ddagger}$ = 41.02 kJ K^{-1} mol^{-1} and $\Delta S^{\ddagger}$ = −36.88 J K^{-1}) calculated for the dynamic process from the line-broadening analysis suggest that the Bailar mechanism is predominant.[30]

Polymerization of Propylene. The polymerization of propylene was performed at room temperature for 3 h in toluene with 30 mL of liquid propylene after the activation of the precatalysts with methylalumoxane as the cocatalyst in a ratio of 1:1000 (M:Al) (Table 1).[18b] Lower MAO amounts did not activate the complexes for the polymerization of propylene (for ethylene *vide infra*).

Table 1. Polymerization of Propylene Promoted by the Amidinate Complexes Activated by MAO

complex	mass of polymer (g)	activity[a] (×10^4)
8	0.86	1.56
9	2.92	4.48
10	1.95	3.03
11	1.12	2.53
12	0.42	0.90
13	0.57	1.33
14	0.41	0.79
15	0.74	1.62
16	0.75	1.72

[a]Activity (g of polymer (mol of catalyst)$^{-1}$ h^{-1}).

When the polymerization reaction was carried for 1 h, only a trace amount of polymer was obtained, indicating the slow rate of activation.

Scheme 3. Reaction of 6a with $HfCl_4$ Showing the Formation of Mono- or Tris(amidinate) Complexes

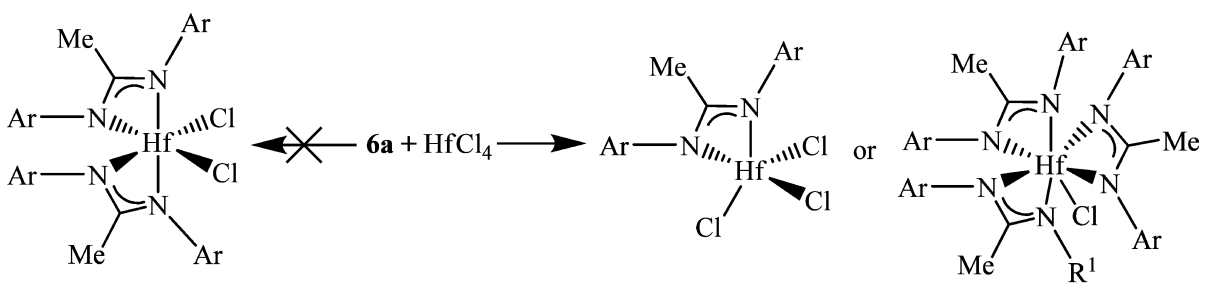

Ar = anisyl

(17)

(18)

dx.doi.org/10.1021/om4006998 | *Organometallics* XXXX, XXX, XXX–XXX

Table 2. Polymerization of Propylene: Heptane-Insoluble Fraction

complex	mass (g)	M_w[a]	M_n[b]	PD[c]	R_i[d]	R_t[e]	*mmmm*[f] (%)	mp[g] (°C)
11	0.42	196 000	65 300	3.0	3.9	2.5	40	143.4
12	0.22	821 000	391 000	2.1	1.8	0.2	27	140.3
13	0.14	225 000	72 600	3.1	1.2	0.7	54	149.9
14	0.12	270 000	90 000	3.0	0.5	0.2	40	150.1
15	0.34	246 000	98 400	2.5	2.7	1.2	42	145.4
16	0.47	497 000	160 300	3.1	3.8	1.0	43	142.8

[a]Molecular weight (g/mol). [b]Number average molecular weight (g/mol). [c]Polydispersity. [d]Rate of monomer insertion (mmol/h). [e]Rate of chain termination (μmol/h). [f]Pentad analysis measured by ^{13}C NMR. [g]Melting point of polymer from the second DSC curve.

After activation with MAO, the catalytic species obtained from the complexes **11**−**16** polymerized propylene, forming two polymeric fractions, which were separated following a Soxhlet extraction in heptane.[32] The heptane-soluble fraction gave an elastomeric polymer, whereas the heptane-insoluble polymer was a stereoregular material. We have shown that the stereoregular fraction is produced by a cationic pseudo-C_2-symmetric bis(κ^2-amidinate) alkyl species, whereas the elastomeric fraction is produced by the corresponding cationic mono(amidinate) dialkyl species.[17] The production of these two fractions will be discussed further as a function of the different active catalysts.

Complex **12** was the unique complex that gives only one insoluble polymeric fraction with a narrow polydispersity, indicating the formation of only one active species. It is important to point out that when MAO was added to a toluene solution of the complex, no precipitate was formed.

The rates of monomer insertion and chain termination for each of the complexes were calculated using eqs 5 and 6, respectively,[18] and were used to compare the catalytic polymerization activity of the complexes.

$$\text{Monomer insertion rate } (R_i) = \frac{m(\text{polymer})\ [\text{g}]}{M_w(\text{monomer})\left[\frac{\text{g}}{\text{mol}}\right] \times \text{time}\ [\text{h}]} \quad (5)$$

$$\text{Chain termination rate } (R_t) = \frac{m(\text{polymer})\ [\text{g}]}{M_n(\text{polymer}) \times \text{time}\ [\text{h}]} \quad (6)$$

Heptane-Insoluble Fractions. All the polymers that were heptane-insoluble (Table 2) exhibit higher molecular weights as compared to the elastomeric fractions with narrow polydispersities, indicating that these fractions are plausibly obtained by a single-site catalytic species.[33] The percentage of the isotactic pentad domains (*mmmm*) ranges from 27% to 54% and melting points from 140.3 to 150.1 °C.

Among the dimethylamido titanium compounds, complex **14**, bearing an ethyl group at the *ipso*-carbon, has the lower monomer insertion rate (R_i) as compared with complexes **12** and **13**, bearing a hydrogen atom and a methyl group at the *ipso*-carbon, respectively. This result indicates that for a series of similar complexes the less bulky substituent at the *ipso*-carbon induces a faster monomer insertion rate. Although the rate of insertion for complex **13** is higher than that of complex **14**, the molecular weight M_n of the polymer obtained with complex **14** is higher than that obtained with complex **13**. Since the molecular weight of a polymer depends on the ratio between the rate of insertion (monomer insertion) and the rate of termination (formation of chains), it is clear that for complex **14** this ratio is larger as compared to complex **13** (2.5×10^3 and 1.7×10^3 for complexes **14** and **13**, respectively).

For the corresponding titanium dichloride complexes **15** and **16**, containing a methyl or an ethyl moiety at the *ipso*-carbon, respectively, the same trend regarding molecular weights is observed; however the trend for the insertion rates is reverse. This result indicates that for complex **16** the ratio R_i/R_t (3.8×10^3) is higher than that of complex **15** (2.3×10^3). For the complexes that are discussed in this article, the reactivity of the amidinate titanium dichloride complexes is higher than that of the corresponding dimethylamido analogues. This result is likely due to a slower activation for the latter as compared to the former complexes. It is worth mentioning that both types of complexes will yield the same cationic entity and consequently similar isotactic polymer fractions. Moreover since there is a large excess of MAO, a minimal effect for the different counterions could be expected. In the dimethylamido complexes **13** and **14**, the polymer termination rate was found to be slower than that of the corresponding dichloride complexes **15** and **16**, indicating the importance of the counterion.[1b,2o,18b,34]

Complex **11**, which bears a hydrogen on the *ipso*-carbon and a cyclohexyl group on each of the amidinate nitrogen atoms, exhibits higher R_i and R_t values as compared to the N-phenyl-substituted complexes (**12**, **13**, and **14**), producing a polymer with a lower molecular weight.

Heptane-Soluble Fraction. As we have shown above, the stereoirregular elastomeric fraction is produced by the corresponding cationic mono(amidinate) dialkyl species formed during the activation with MAO.[17] When comparing the elastomeric fraction obtained by complexes **13** and **14**, we observed that the complex with the ethyl-substituted ligands at the *ipso*-position (complex **14**) induced the formation of a polymer with a higher molecular weight as compared to the polymer obtained with complex **13** (Table 3). In addition, the polymerization activity, rate of monomer insertion, and the rate of chain termination exhibited by complex **13** are larger than that of complex **14**. The same trend of a polymer with a higher molecular weight, a lower activity, and lower rates for monomer insertion and chain termination is observed for the ethyl-*ipso*-substituted complex **16** as compared to the methyl-*ipso*-substituted complex **15**. The larger coordinative unsaturation of the cationic mono(amidinate) active species plausibly induces the larger activation rates as compared to the corresponding bis(amidinate) species. When comparing the complexes presented in Tables 2 and 3, the mono(amidinate) complex that is generated from complex **11** exhibits the larger activity and the higher insertion and termination rates plausibly due to its large coordinative unsaturation.

Polymerization of Ethylene. The polymerization of ethylene was performed in toluene after the activation of the

dx.doi.org/10.1021/om4006998 | *Organometallics* XXXX, XXX, XXX−XXX

Table 3. Polymerization of Propylene: Heptane-Soluble Fraction

complex	mass (g)	M_w[a]	M_n[b]	PD[c]	R_i[d]	R_t[e]	*mmmm*[f] (%)
8	0.86	105 000	17 200	6.1	6.8	16.5	15
9	2.92	55 000	12 800	4.3	23.0	76.1	12
10	1.95	67 700	20 900	3.2	15.4	31.1	13
11	0.90	32 500	13 000	2.5	8.8	28.3	10
13	0.43	16 800	7000	2.4	3.6	21.5	11
14	0.29	23 800	8800	2.7	1.9	9.1	15
15	0.40	19 800	9000	2.2	3.2	15.0	10
16	0.28	41 500	14 800	2.8	2.2	6.2	18

[a]Molecular weight (g/mol). [b]Number average molecular weight (g/mol). [c]Polydispersity. [d]Rate of monomer insertion (mmol/h). [e]Rate of chain termination (μmol/h). [f]Pentad analysis measured by ^{13}C NMR.

precatalysts with MAO in a 1:1000 (M:Al) ratio, under constant pressure of ethylene (9.86 atm) at room temperature for 0.5 h,[14f] and the results are presented in Table 4.

The generated cationic species, in all cases, produced high-density polyethylene with narrow polydispersities. Precatalyst **12**, with the hydrogen atom at the *ipso*-position of the amidinate ligand, induces the formation of a high molecular weight polyethylene due to the larger rate of insertion as compared to the rate of chain termination. When comparing the polymerization activity obtained using complexes **13** and **14** or **15** and **16** as precatalysts, the complexes possessing a methyl substituent at the *ipso*-position of the amidinate were found to be slightly more active than those with the corresponding ethyl moieties. Regarding the molecular weights, the ratio of R_i/R_t for complex **13** ($R_i/R_t = 4.8 \times 10^3$) is lower than that of complex **14** ($R_i/R_t = 12.6 \times 10^3$), resulting in a lower molecular weight polyethylene. The opposite was observed for the dichloride complexes **15** ($R_i/R_t = 12.2 \times 10^3$) and **16** ($R_i/R_t = 2.4 \times 10^3$), which resulted in the formation of a low molecular weight polymer for the latter complex, due to the high rate of termination.

When the polymerization of ethylene was performed with complex **15** in a 1:500 and 1:100 ratio of catalyst to MAO, at the same experimental conditions, smaller amounts of polymer were obtained (activity: 6.6×10^3 and 0.81×10^3 (g mol^{-1} h^{-1} atm^{-1}), respectively), indicating the dependence of the activity of the complexes on the cocatalyst concentration.

Similarly, in the formation of polyethylene, the activity and the rate of monomer insertion obtained using the precatalyst **11** were found to be the largest, as was also observed in the formation of polypropylene.

It is interesting to point out that the presence of a bulkier substituent at the *ipso*-position of the amidinate ligand, in all presented bis(amidinate) complexes, induced lower activities and lower insertion rates (H > Me > Et). This result is intriguing, as the ethyl group is not expected to be in close proximity to the cationic active site. A close investigation of the X-ray structure of complex **16** shows that the N-phenyl rings are restricted in their rotation and will consequently dispose the aromatic ring in such a manner that the methoxy group will point toward the metal either in the catalyst or at the MAO. This interaction is presumed to inhibit the rapid insertion as was found for similar complexes containing the H/Me groups at the same position or as compared with the cyclohexyl moiety in complex **11**.

The titanium mono(amidinate) complexes (**8**, **9**, and **10**) exhibit good catalytic activity after their activation with MAO in the polymerization of ethylene and propylene, producing high-density polyethylene or elastomeric polypropylene (soluble in hot heptane; *mmmm* = 12−15%), respectively.[17,18] Interestingly, in these complexes, a profound steric influence of the amidine carbon and N-phenyl substituents on the rate of monomer insertion and rate of chain termination was observed. The independently prepared hafnium mono- and tris-(amidinate) chloride complexes were tested for their catalytic activity in polymerization reactions. The mono(amidinate) complex **17** was found to be highly active (16.2×10^3 and 27.0×10^3 g mol^{-1} h^{-1} atm^{-1} for ethylene and propylene, respectively), whereas the corresponding tris(amidinate) complex **18** was inactive.

Radical Trapping Experiments. In order to understand the polymerization mechanism and the nature of the active catalytic species formed during the reaction, complex **15** was mixed with MAO (1:100) in a sealed NMR tube with toluene-d_8; a precipitate was promptly formed, and the ESR data of the samples were measured. A broad asymmetrical ESR signal was observed, indicating the formation of agglomerates containing paramagnetic Ti(III) species.[17b]

Only the precipitate was found to be EPR active, whereas the mother liquor did not produce any ESR signal, indicating the absence of Ti(III) species in solution.

To elucidate the nature of the Ti(III) in the reaction mixture, the reaction of complex **15** and MAO (1:100) was performed with the addition of C_{60} as a radical trapping agent.[35]

As it is expected that a methyl radical formed during the reaction will be trapped by C_{60}, visible light (λ > 500 nm) was used at the ESR cavity to observe the reversible dissociation of the dimer of the fullerenyl radical (eq 7).

Table 4. Data for the Polymerization of Ethylene Promoted by the Amidinate Complexes Activated by MAO

complex	mass (g)	A[a] ($\times 10^3$)	M_w[b]	M_n[c]	PD[d]	R_i[e]	R_t[f]	mp[g] (°C)
8	0.29	3.19	261 000	104 400	2.5	20.4	5.5	138.4
9	0.96	8.95	391 000	150 400	2.6	68.5	12.8	137.2
10	0.87	8.36	236 600	43 000	5.5	62.0	40.4	137.3
11	0.90	11.79	690 400	460 300	1.5	75.2	4.6	139.2
12	0.13	1.78	1016 000	564 400	1.8	9.7	0.5	138.2
13	0.53	7.49	406 000	135 300	3.0	39.0	8.1	140.3
14	0.53	6.25	745 000	354 800	2.1	31.2	2.5	137.8
15	0.86	11.49	687 000	343 500	2.0	61.5	5.0	132.3
16	0.46	6.40	203 100	67 700	3.0	32.8	13.6	135.0

[a]Activity (g of polymer) × (mol of catalyst^{-1} h^{-1} atm^{-1}). [b]Molecular weight (g/mol). [c]Number average molecular weight (g/mol). [d]Polydispersity. [e]Rate of monomer insertion (mmol/h). [f]Rate of chain termination (μmol/h). [g]Melting point of polymer from the second DSC curve.

dx.doi.org/10.1021/om4006998 | *Organometallics* XXXX, XXX, XXX−XXX

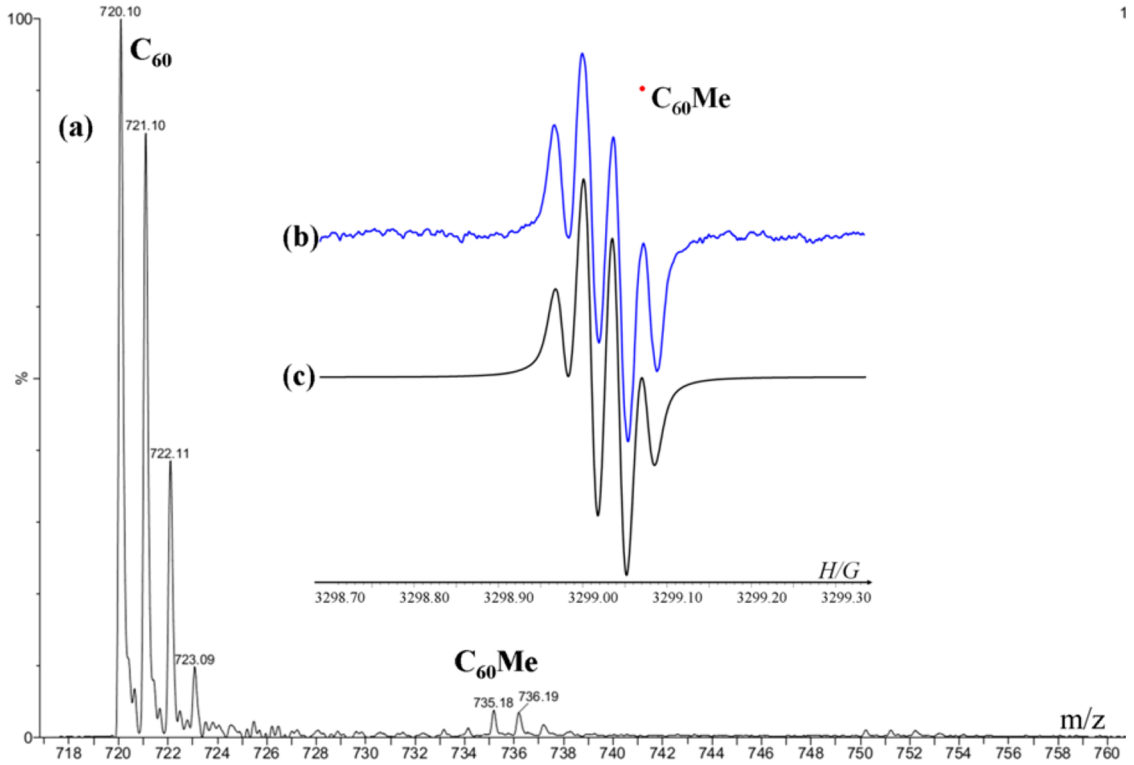

Figure 6. MALDI-TOF analysis of the sample prepared from complex **15** and MAO using fullerene as radical trapping agent. Catalyst added in a ratio of complex **15**:MAO 1:100; (a) MALDI-TOF spectrum of the reaction precipitate; (b) ESR spectrum of the reaction mixture at high resolution (a_H(3H) = 0.035 G) under visible light irradiation (λ > 550 nm); (c) simulated spectrum of $^{\bullet}C_{60}Me$.

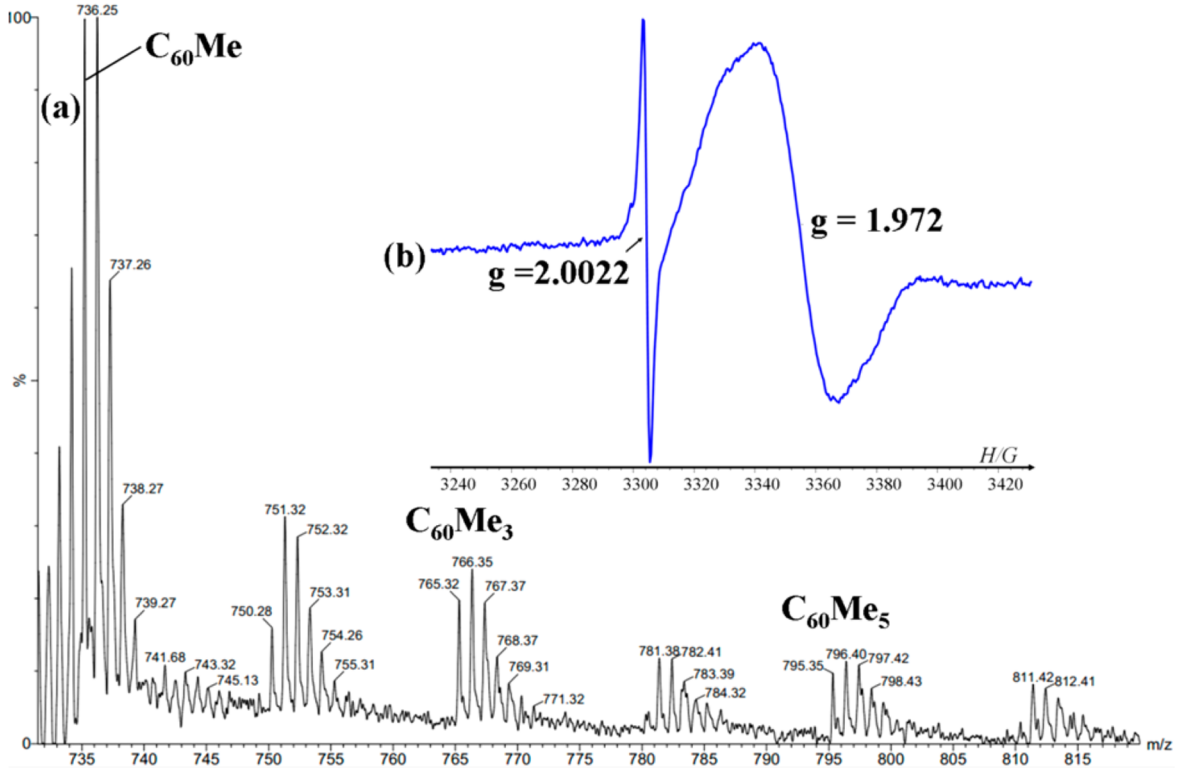

Figure 7. MALDI-TOF analysis of sample prepared from complex **15** and MAO using fullerene as radical trapping agent after backfilling with ethylene. Catalyst added in a ratio of complex **15**:MAO 1:100. (a) MALDI-TOF spectrum of the solid part of catalytic slurry. (b) ESR spectrum of the reaction mixture shows stable adduct of multiple additions of Me-radical to C_{60} (g = 2.0022) and paramagnetic agglomerate of Ti(III) and MAO (g = 1.972).

dx.doi.org/10.1021/om4006998 | *Organometallics* XXXX, XXX, XXX–XXX

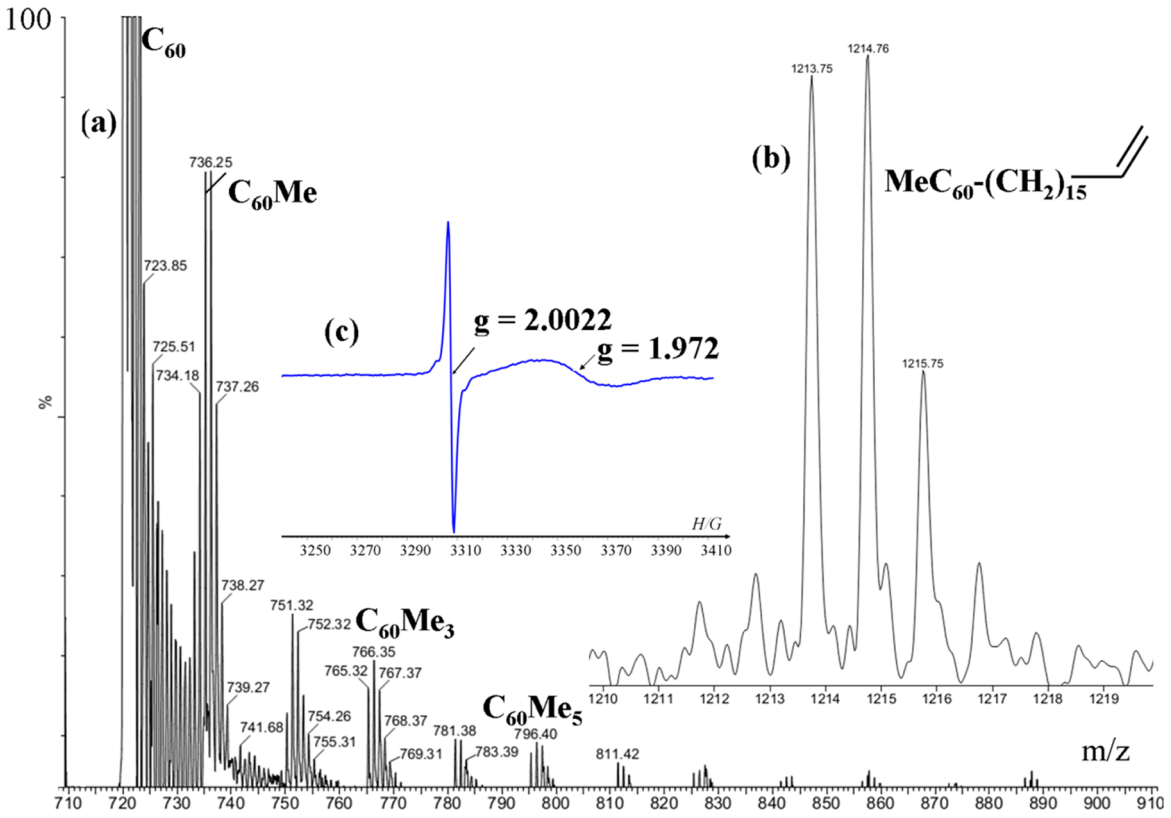

Figure 8. MALDI-TOF analysis of sample prepared from complex **15** and MAO using fullerene as radical trapping agent after backfilling with ethylene. Catalyst added in a ratio of complex **15**:MAO 3:100. (a) MALDI-TOF spectrum of the solid part of the catalytic slurry. (b) Enlargement of the signal that corresponds to the highest mass. (c) ESR spectrum of the reaction mixture.

$$MeC_{60}-C_{60}Me \rightleftharpoons 2\,{}^{\bullet}C_{60}Me \quad (7)$$

The ESR spectrum showed a characteristic signal for the ${}^{\bullet}C_{60}Me$ radical (Figure 6), which was further supported by the respective ions at 735 for the ${}^{\bullet}C_{60}Me$ radical and 736 for $HC_{60}Me$ in MALDI-TOF analysis, indicating the formation of the methyl radical via the reduction of the dimethyl Ti(IV) complex with MAO, producing the Ti(III) species. It is important to note that the reaction between MAO and C_{60} does not produce the ${}^{\bullet}C_{60}Me$ radical.

When an aliquot of ethylene was added to the catalytic mixture, unlike in the previous experiments,[17b,36] no decrease of the Ti(III) species was observed, even after multiple additions of ethylene. However, it was seen that multiple methyl radical fragments were trapped by a single fullerene molecule (Figure 7), but the trapping of polyethylene chains was not seen at the ratio of catalyst to MAO of 1:100. Interestingly, when the catalyst loading was increased to 3:100, a decrease in the Ti(III) species was observed after multiple additions of ethylene. In addition, multiple additions of methyl radicals on fullerene were observed, as well as a polyethylene chain containing 17 monomer units attached to C_{60} (Figure 8). Furthermore, we see that if the catalyst loading is increased further, reaching the ratio of 10:100, no polymer chain-substituted fullerene was observed.

On the basis of the results presented above and by comparison to similar studies reported earlier,[17b,36] a catalytic cycle is proposed (Scheme 4). The starting Ti(IV) complex **a** is reduced by MAO to form the corresponding Ti(III) complex **b** producing a methyl radical, which was trapped by C_{60} (Figure 7). Complex **b** reacts with ethylene, reoxidazing the Ti(III) to Ti(IV) and producing the corresponding complex **c** bearing a radical alkyl chain. Additional ethylene insertions will form complex **d**. An expected β-H elimination of the radical chain will form the Ti(IV)-hydride complex (**e**), and the oligomeric alkyl radical chain will be trapped by C_{60} (Figure 8b and c). The Ti(IV) hydride complex plausibly undergoes a metathesis with MAO, regenerating the Ti(IV) catalyst **a**. The regeneration of complex **a** is proposed based on the additional methyl radicals that can be trapped by one molecule of C_{60}, which is observed only after the addition of ethylene (Figure 8a).

The parallel reaction of complex **a** with MAO forms the corresponding cationic complex **f**, which will be the active species for the observed polymerization of ethylene.

CONCLUSIONS

Various group 4 complexes were prepared with amidines bearing electron-donating and/or -coordinating substituents at the nitrogen moiety. The steric properties of the ligands were tuned in order to prepare the mono- and bis(amidinate) complexes. In solution, the complexes exhibit fluxional behavior. The polymerization of propylene, promoted by bis(amidinates), after their activation with MAO, provided two polymeric fractions. All the obtained heptane-soluble polymers were elastomeric in nature with low molecular weights, whereas the insoluble polymers were slightly to moderately stereoregular with *mmmm* ≈ 27−54%. In the polymerization of ethylene, all the complexes yield a high-density polyethylene.

Interestingly, a noticeable influence of the amidine *ipso*-substituent on the activity of the catalyst and properties of the obtained polymer was observed. The presence of a bulkier substituent at the *ipso*-position of the amidinate ligand induced

dx.doi.org/10.1021/om4006998 | *Organometallics* XXXX, XXX, XXX−XXX

Scheme 4. Plausible Mechanism for Polymerization of Ethylene Catalyzed by a Titanium(IV) Complex

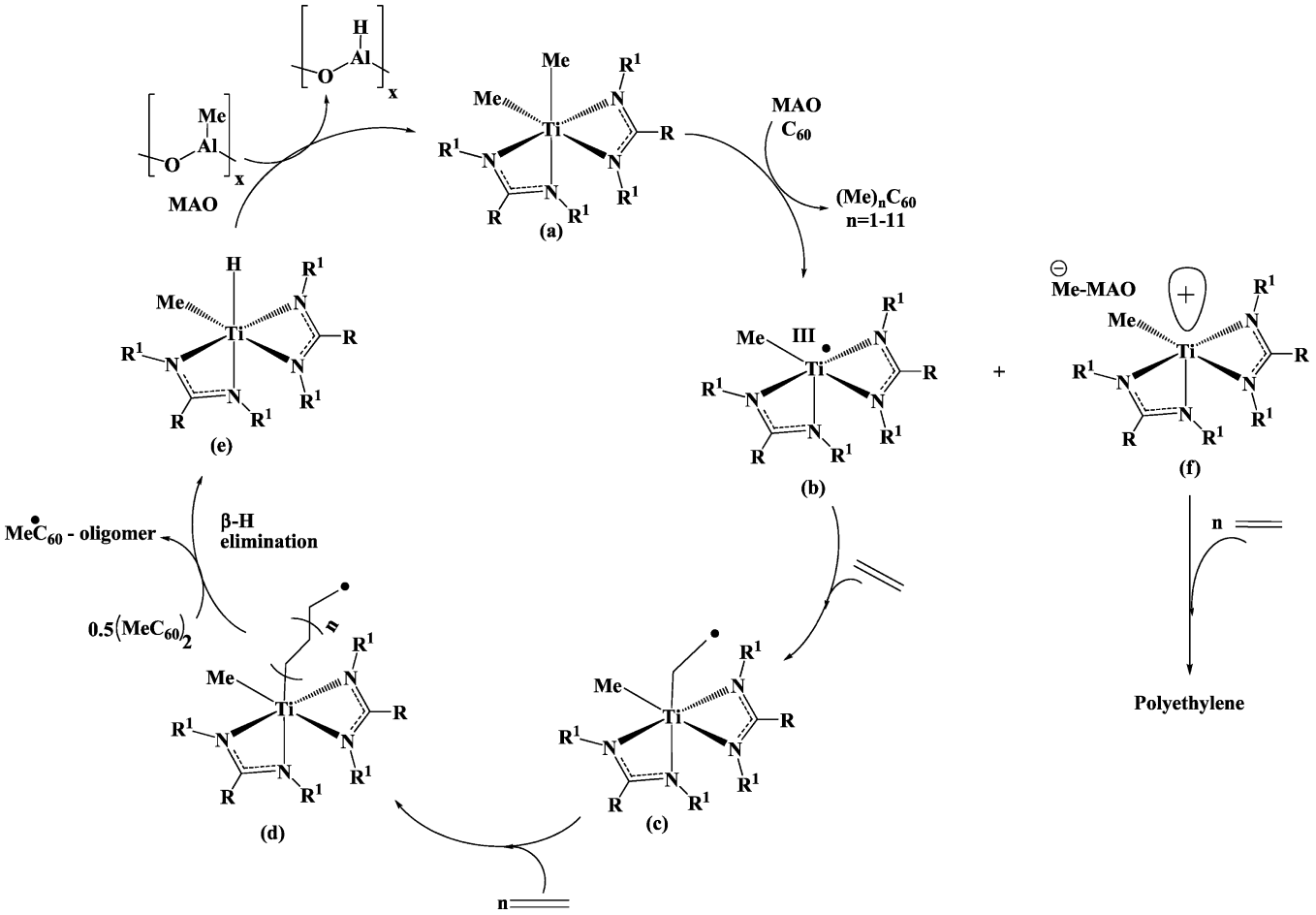

lower activities and lower monomer insertion rates (H > Me > Et). Considering the distant location of the *ipso*-substituent from the active metal center in the κ^2-bonded amidinate, this result is quite remarkable. By close investigation of the structural features of the *ipso*-ethyl-substituted complex (**14**) it is envisaged that, due to the steric hindrance induced by the ethyl group, the N-phenyl rings are not able to freely rotate. Hence, the aromatic rings will be posed with the methoxy group pointing toward either the metal center or MAO and presumably impeding the rapid monomer insertion as compared to similar complexes containing the smaller H/Me groups at the same position.

The highest activity observed by complex **11** as compared to all the bis(N-anisyl)-substituted titanium complexes indicates the plausible methoxide interaction with the metal center, reducing the polymerization activity of the latter complexes.

All the mono(amidinate) complexes exhibit good activity in the polymerization of ethylene and propylene, producing high-density polyethylene and elastomeric polypropylene. The steric effect of the amidine *ipso*-carbon and N-phenyl substituents on the polymerizations was observed and follows the same trend as in the corresponding bis(amidinates).

In addition, a plausible mechanism for the polymerization, indicating the nature of the catalytic species, is presented using a combination of ESR, C_{60} trapping radical, and MALDI-TOF experiments.

EXPERIMENTAL SECTION

All manipulations of air-sensitive materials were performed with the exclusion of oxygen and moisture in flamed Schlenk-type glassware on a dual-manifold Schlenk line or interfaced to a high-vacuum (10^{-5} Torr) line, or in a nitrogen-filled M-Braun glovebox with a medium-capacity recirculator (1−2 ppm O_2).

Argon and nitrogen gases were purified by passage through a MnO oxygen-removal column and a Davison 4 Å activated molecular sieve column. All the common and deuterated solvents (THF, toluene, hexane, and toluene-d_8) were distilled and stored over Na/K alloy.

The NMR spectra were recorded on Bruker AM 300 and AM 500 spectrometers. Chemical shifts for ^{1}H and ^{13}C were referenced to internal solvent resonances and are reported relative to TMS. NMR experiments for the air-sensitive metal complexes were conducted on Teflon valve-sealed tubes (J-Young) after vacuum transfer of the solvent in a high-vacuum line. The NMR experiments for polypropylene (in tetrachloroethylene-d_2 (TCE)) and polyethylene (in 1,2,4-trichlorobenzene with DMSO-d_6 capillary) were carried at 363 K on a 300 MHz or 500 MHz NMR spectrometer.

The single-crystal material was immersed in Paratone-N oil and was quickly fished with a glass rod and mounted on a Kappa CCD diffractometer under a cold stream of nitrogen. Data collection was performed using monochromated Mo Kα radiation using φ and ω scans to cover the Ewald sphere.[37] Accurate cell parameters were obtained with the amount of indicated reflections (Supporting Information).[38] The structure was solved by SHELXS-97 direct methods[39] and refined by the SHELXL-97 program package.[40] The atoms were refined anisotropically. Hydrogen atoms were included using the riding model. Mercury 3.1[41] software was used for molecular graphics. The cell parameters and refinement data are presented in the Supporting Information.

dx.doi.org/10.1021/om4006998 | *Organometallics* XXXX, XXX, XXX−XXX

Melting points of the polymers were measured by DSC (Polymer Laboratories, UK) from the second heating thermogram (heating rate:10 °C/min). Molecular weights and polydispersities of polymers were determined by the GPC method on the Waters-Alliance 2000 instrument using 1,2,4-trichlorobenzene as a mobile phase at 160 °C. Polystyrene standards were used for the standard calibration curve of the GPC. Elemental analysis of all the compounds was carried out on a Flash 2000 CHNS analyzer.

MALDI-TOF LD+ and LD− experiments were performed on a Waters MALDI Micromass MX spectrometer using the standard Micromass 96-well matrix along with fullerene, which has a higher ability for light absorption and ionization than Ag. Mass analyzing was performed in the reflectron mode in the region between 300 and 3000. ESR spectra were recorded on a Bruker EMX-10/12 X-band (ν = 9.4 GHz) digital ESR spectrometer. All spectra were recorded at a microwave power of 10−1 mW and a 100 kHz magnetic field modulation of 1.0−0.5 G amplitude. Digital field resolution was 2048 points per spectrum, allowing all hyperfine splitting to be measured directly with accuracy better than 0.2 G. Spectral processing and simulation were performed with Bruker WIN-EPR and SimFonia software. A standard TEMPO solution (10^{-3} M) was used for an estimation of the number of radicals in the catalytic mixture (no. of radicals = 1.7×10^{18}).

All of the anilines, orthoesters, and $ZrCl_4$ were purchased from Sigma-Aldrich; $HfCl_4$ was purchased from Strem Chemicals. All the chemicals were used without further purification unless otherwise stated. $TiCl_4{\cdot}2THF$,[42] $ZrCl_4{\cdot}2THF$,[42] $Ti(N(CH_3)_2)_4$,[43] and ligands [(2,6-(CH(CH$_3$)$_2$)$_2$C$_6$H$_3$)NC(H)NH(2,6-(CH(CH$_3$)$_2$)$_2$C$_6$H$_3$)] (**1**), [(2,4,6-(CH$_3$)$_3$C$_6$H$_2$)NC(H)NH(2,4,6-(CH$_3$)$_3$C$_6$H$_2$)] (**2**),[26] [(2,4,6-(CH$_3$)$_3$C$_6$H$_2$)NC(CH$_3$)NH(2,4,6-(CH$_3$)$_3$C$_6$H$_2$)] (**3**), [(C$_6$H$_{11}$)NC(H)NH(C$_6$H$_{11}$)] (**4**),[20] [(2-OCH$_3$C$_6$H$_5$)NC(H)NH(2-OCH$_3$C$_6$H$_5$)] (**5**),[44] and [(2-OCH$_3$C$_6$H$_5$)NC(CH$_3$)NH(2-OCH$_3$C$_6$H$_5$)] (**6**)[20] were prepared by the literature procedures.

[(2-OCH$_3$C$_6$H$_5$)NC(C$_2$H$_5$)NH(2-OCH$_3$C$_6$H$_5$)] (7). Ligand **7** was prepared by following a method similar to the procedure reported by Taylor.[20] A mixture of 8.81 g (0.05 mol) of triethylorthopropionate, 12.3 g (0.10 mol) of *o*-anisidine, and 3.0 g (0.05 mol) of glacial acetic acid was heated and refluxed at 140 °C for 4 h. After that period of time the temperature was raised to 150 °C, and ethanol was distilled off. The remaining viscous liquid was treated with an aqueous solution of sodium carbonate (10%, 100 mL), then extracted with diethyl ether (50 mL). The aqueous layer was washed with three additional portions of ether (20 mL × 3). Organic fractions were combined, dried over Na_2SO_4, and evaporated under reduced pressure to yield a crude compound as a white solid. Recrystallization from EtOH/H_2O (70:30, 100 mL) yielded pure amidine **7** as colorless crystals. Yield: 92%. Mp: 74−76 °C. ^{1}H NMR ($CDCl_3$, 400 MHz, 296 K): δ 8.79 (1H, s, N*H*), 7.06−6.85 (8H, m, aromatic), 3.92 (3H, s, OC*H*$_3$), 3.81 (3H, s, OC*H*$_3$), 2.28 (2H, q, J = 7.6 Hz, C*H*$_2$CH$_3$), 1.17 (3H, t, J = 7.6 Hz, CH$_2$C*H*$_3$). ^{13}C NMR: 157.5 (N*C*N), 149.6 (*C*-OMe), 139.2 (*C*-NCN), 122.7, 121.1, 119.2, 111.2 (*C*-aromatic), 55.72 (O*C*H$_3$). 25.8 (*C*H$_2$CH$_3$), 11.7 (CH$_2$*C*H$_3$). Anal. Calcd for $C_{17}H_{20}N_2O_2$: C, 71.81; H, 7.09; N, 9.85. Found: C, 71.92; H, 6.98; N, 9.96.

[HC(N(2,6-(CH(CH$_3$)$_2$)$_2$C$_6$H$_3$))$_2$]Ti[N(Me$_2$)]$_3$ (8). A toluene solution of $Ti(NMe_2)_4$ (0.23 g, 0.001 mol) was added dropwise to a stirred solution of **1** (0.364 g, 0.001 mol) in toluene at room temperature, and the resulting red-orange solution was stirred overnight. All volatiles were evaporated to yield complex **8** as an orange solid. X-ray quality crystals were obtained by slow evaporation of a hexane solution of **8**. Yield: 91%. ^{1}H NMR (toluene-d_8, 300 MHz, 298 K): δ 7.63 (1H, s, NC*H*N), 7.10 (6H, m, aromatic), 3.49 (4H, sept, J = 6.6 Hz, C*H*(CH$_3$)$_2$), 3.12 (18H, s, N(CH$_3$)$_2$), 1.23 (24H, d (J = 6.6 Hz), CH(C*H*$_3$)$_2$). ^{13}C NMR: 165.7 (N*C*N), 143.5 (*C*-NCN), 136.9, 124.9, 122.9 (*C*-aromatic), 45.4 (N(*C*H$_3$)$_2$), 27.3 (*C*H(CH$_3$)$_2$), 24.3 (CH(*C*H$_3$)$_2$). Anal. Calcd for $C_{31}H_{54}N_5Ti$: C, 68.36; H, 9.99; N, 12.86. Found: C, 67.83; H, 9.51; N; 12.76.

[HC(N(2,4,6-(CH$_3$)$_3$C$_6$H$_2$))$_2$]Ti[N(Me$_2$)]$_3$ (9). Similar to the procedure described for **8**, 0.28 g (0.001 mol) of **2** and 0.23 g (0.001 mol) of $Ti(NMe_2)_4$ were reacted in toluene to yield complex **9** as an orange solid. X-ray quality crystals were obtained by slow evaporation of a toluene solution of **9**. Yield: 92%. ^{1}H NMR (toluene-d_8, 300 MHz, 298 K): δ 7.33 (1H, s, NC*H*N), 6.84 (4H, s, aromatic), 3.15 (18H, s, N(CH$_3$)$_2$), 2.28 (12H, s, *o*-CH$_3$), 2.22 (6H, s, *p*-CH$_3$). ^{13}C NMR: 167.5 (N*C*N), 144.4 (*C*-NCN), 136.9, 132.0, 128.7 (*C*-aromatic), 45.2 (N(*C*H$_3$)$_2$), 19.9 (*o*-*C*H$_3$), 19.3 (*p*-*C*H$_3$). Anal. Calcd for $C_{25}H_{42}N_5Ti$: C, 65.20; H, 9.19; N, 15.21. Found: C, 64.50; H, 9.82; N, 14.81.

[CH$_3$C(N(2,4,6-(CH$_3$)$_3$C$_6$H$_2$))$_2$]Ti[N(Me$_2$)]$_3$ (10). The same procedure as for complex **8** was employed. X-ray quality crystals were obtained by slow evaporation of a hexane solution of **10**. Yield: 90%. ^{1}H NMR (toluene-d_8, 300 MHz, 298 K): δ 6.98 (4H, s, aromatic), 3.24 (18H, s, N(C*H*$_3$)$_2$), 2.36 (12H, s, *o*-C*H*$_3$), 2.32 (6H, s, *p*-C*H*$_3$), 1.35 (C*H*$_3$). ^{13}C NMR: 170.5 (N*C*N), 145.4 (*C*-NCN), 136.4, 131.0, 127.9 (*C*-aromatic), 45.6 (N(*C*H$_3$)$_2$), 20.1 (*o*-*C*H$_3$), 19.5 (*p*-*C*H$_3$), 19.1 (*C*H$_3$). Anal. Calcd for $C_{26}H_{44}N_5Ti$: C, 65.81; H, 9.35; N, 14.76. Found: C, 65.41; H, 9.82; N, 14.92.

[HC(N(C$_6$H$_{11}$))$_2$]$_2$Ti[N(Me$_2$)]$_2$ (11). A toluene solution of $Ti(NMe_2)_4$ (0.23 g, 0.001 mol) was added dropwise to a stirred solution of **4** (0.41 g, 0.002 mol) in toluene (30 mL) at room temperature. The dark red solution was allowed to stir overnight at room temperature, followed by removal of toluene *in vacuo* to yield a dark red residue. The residue was dissolved in hexane (10 mL) and evacuated again to obtain the pure complex **11** as dark red solid. Yield: 88%. ^{1}H NMR (toluene-d_8, 300 MHz, 296 K): δ 7.95 (1H, s, NC*H*N), 3.43 (12 H, s, N(CH$_3$)$_2$), 3.12 (4H, m, Cy-H_{ipso}), 1.95−1.08 (40 H, m, Cy-H). ^{13}C NMR: 161.1 (N*C*N), 60.7 (*C*-NCN), 48.3 (N(*C*H$_3$)$_2$), 35.7, 26.0 (*C*-Cy). Anal. Calcd for $C_{30}H_{60}N_6Ti$: C, 65.19; H, 10.94; N, 15.21. Found: C, 64.37; H, 10.63; N, 14.80.

[HC(N(2-OCH$_3$C$_6$H$_5$))$_2$]$_2$Ti[N(Me$_2$)]$_2$ (12). The same procedure as described above was followed, but the reaction time was reduced to 1 h. Yield: 92%. ^{1}H NMR (toluene-d_8, 300 MHz, 296 K): δ 9.40 (1H, s, NC*H*N), 7.48 (4H, d, J = 6 Hz, *o*-*H* aromatic), 6.92−6.83 (8H, m, aromatic), 6.57 (4H, d, J = 6 Hz, *m*-*H* aromatic), 3.39 (12H, s, OC*H*$_3$), 3.18 (12H, s, N(C*H*$_3$)$_2$). ^{13}C NMR: 164.9 (N*C*N), 152.2 (*C*-NCN), 137.5, 124.7, 122.3, 120.9, 111.4 (*C*-aromatic *C*), 54.5 (O*C*H$_3$), 46.7 (N(*C*H$_3$)$_2$). Anal. Calcd for $C_{34}H_{44}N_6O_4Ti$: C, 62.96; H, 6.84; N, 12.96. Found: C, 61.55; H, 6.18; N, 11.66.

[CH$_3$C(N(2-OCH$_3$C$_6$H$_5$))$_2$]$_2$Ti[N(Me$_2$)]$_2$ (13). The same procedure for the preparation of **11** was followed. Yield: 90%. ^{1}H NMR (toluene-d_8, 300 MHz, 298 K): δ 7.28 (4H, d, J = 5.8 Hz, *o*-*H* aromatic), 7.01−6.69 (8H, m, aromatic), 6.65 (4H, d, J = 5.8 Hz, *m*-*H* aromatic), 3.39 (12H, s, OC*H*$_3$), 3.32 (12H, s, N(C*H*$_3$)$_2$), 1.74 (6H, s, C*H*$_3$). ^{13}C NMR: 171.6 (N*C*N), 153.4 (*C*-NCN), 138.3, 136.9, 123.4, 120.4, 111.1 (*C*-aromatic), 54.3 (O*C*H$_3$), 46.8 (N(*C*H$_3$)$_2$), 14.4 (*C*H$_3$). Anal. Calcd for $C_{36}H_{48}N_6O_4Ti$: C, 63.90; H, 7.15; N, 12.42. Found: C, 63.25; H, 6.97; N, 11.81.

[C$_2$H$_5$C(N(2-OCH$_3$C$_6$H$_5$))$_2$]$_2$Ti[N(Me$_2$)]$_2$ (14). The same procedure for the preparation of **11** was followed. X-ray quality crystals were obtained by slow evaporation of a hexane/toluene (1:1) solution. Yield: 90%. ^{1}H NMR (toluene-d_8, 300 MHz, 298 K): δ 7.30 (4H, d, J = 6.3 Hz, *o*-*H* aromatic), 6.97−6.86 (8H, m, aromatic), 6.62 (4H, d, J = 6.3 Hz, *m*-*H* aromatic), 3.37 (12H, s, OCH$_3$), 3.27 (12H, s, N(CH$_3$)$_2$), 2.20 (2H, q, J = 7.5 Hz, C*H*$_2$CH$_3$), 0.78 (3H, t, J = 7.5 Hz, CH$_2$C*H*$_3$). ^{13}C NMR: 174.9 (N*C*N), 153.44 (*C*-NCN), 138.3, 136.9, 123.4, 120.2, 110.7 (*C*-aromatic), 54.18 (O*C*H$_3$), 46.7 (N(*C*H$_3$)$_2$), 22.1 (*C*H$_2$CH$_3$), 10.1 (CH$_2$*C*H$_3$). Anal. Calcd for $C_{38}H_{52}N_6O_4Ti$: C, 64.76; H, 7.44; N, 11.93. Found: C, 64.11; H, 7.77; N, 11.53.

[CH$_3$C(N(2-OCH$_3$C$_6$H$_5$))$_2$]$_2$TiCl$_2$ (15). A ^{n}BuLi solution (1.25 mL, 1.6 M in hexane) was added dropwise to a solution of ligand **6** (0.54 g, 0.002 mol) in THF at −78 °C under nitrogen flow. The solution was allowed to slowly warm to room temperature and stirred overnight to obtain the lithium salt **6a**. This solution was cooled to −78 °C, and a slurry of $TiCl_4{\cdot}2THF$ (0.34 g, 0.001 mol) in toluene was added dropwise. The reaction mixture was brought to room temperature and stirred overnight. The solvents were removed under vacuum to obtain a solid residue. To this residue was added 30 mL of toluene, and the resulting suspension was filtered. The filtrate was concentrated, and hexane was added slowly to the solution, causing a precipitation of **15**. The heterogeneous solution was filtered, and the resulting solid was washed with hexane (3 × 10 mL) and dried under vacuum to afford pure complex as a dark brown solid. Yield: 80%. ^{1}H NMR (toluene-d_8,

dx.doi.org/10.1021/om4006998 | Organometallics XXXX, XXX, XXX−XXX

500 MHz, 298 K): δ 7.52 (4H, d, J = 8 Hz, *o-H* aromatic), 7.00−6.83 (8H, m, aromatic), 6.61 (4H, d, J = 8 Hz, *m-H* aromatic), 3.37 (12H, s, OCH_3), 1.63 (6H, s, CH_3). ^{13}C NMR: 173.1 (NCN), 146.7 (*C*-NCN), 131.7, 123.8, 122.4, 115.6, 106.7 (*C*-aromatic), 50.1 (OCH_3), 9.44 (CH_3). Anal. Calcd for $C_{32}H_{36}Cl_2N_4O_4Ti$: C, 58.28; H, 5.50; N, 8.50. Found: C, 57.84; H, 5.41; N, 8.30.

$[C_2H_5C(N(2\text{-}OCH_3C_6H_5))_2]_2TiCl_2$ (16). Similar to the above procedure, the lithium salt **7a** was prepared *in situ* by reacting 0.568 g (0.002 mol) of **7** with 1.25 mL of ^{n}BuLi (1.6 M in hexane) in THF. The resulting solution of **7a** was then reacted with 0.34 g (0.001 mol) of $TiCl_4$·2THF to obtain complex **16** as dark brown solid. Yield: 80%. ^1H NMR (toluene-d_8, 300 MHz, 298 K): δ 7.46 (4H, J = 6 Hz, *o-H* aromatic), 7.12−6.79 (8H, m, aromatic), 6.57 (4H, d, J = 6 Hz, *m-H* aromatic), 3.38 (12H, s, OCH_3), 2.12 (4H, q, J = 7.6 Hz, CH_2CH_3), 0.69 (6H, t, J = 7.6 Hz, CH_2CH_3). ^{13}C NMR: 181.2 (NCN), 151.8 (*C*-NCN), 136.9, 127.4, 125.8, 120.4, 111.5 (*C*-aromatic), 55.1 (OCH_3), 22.2 (CH_2CH_3), 9.27 (CH_2CH_3). Anal. Calcd for $C_{34}H_{40}Cl_2N_4O_4Ti$: C, 59.40; H, 5.86; N, 8.15. Found: C, 59.69; H, 6.15; N, 7.86.

$[CH_3C(N(2\text{-}OCH_3C_6H_5))_2]HfCl_3$ (17). Similar to the above procedure, the lithium salt **6a** was prepared *in situ* by reacting 0.54 g (0.002 mol) of **6** with 1.25 mL of ^{n}BuLi (1.6 M in hexane) in THF overnight. To the resulting solution of **6a** was added slowly a slurry of 0.32 g (0.001 mol) of $HfCl_4$ in toluene at −78 °C. The mixture was stirred overnight at room temperature to obtain complex **17** as a light yellow solid. ^1H NMR (C_6D_6, 300 MHz, 298 K): δ 7.15 (2H, d, J = 6 Hz, *o-H* aromatic), 6.72−6.62 (4H, m, aromatic), 6.19 (2H, d, J = 6 Hz, *m-H* aromatic), 3.61 (6H, s, OCH_3), 1.65 (3H, s, CH_3). Anal. Calcd for $C_{16}H_{16}Cl_3HfN_2O_2$: C, 34.68; H, 3.09; N, 5.06; Cl, 19.19. Found: C, 33.26; H, 3.78; N, 4.44; Cl, 21.78.

$[CH_3C(N(2\text{-}OCH_3C_6H_5))_2]_3HfCl$ (18). Similar to the above procedure, the lithium salt **6a** was prepared *in situ* by reacting 0.54 g (0.002 mol) of **6** with 1.25 mL of ^{n}BuLi (1.6 M in hexane) in THF overnight. The resulting suspension of **6a** was then added dropwise to a stirring suspension of 0.32 g (0.001 mol) of $HfCl_4$ in THF at −78 °C. The mixture was allowed to stir overnight at room temperature. After that period of time all volatiles were removed under reduced pressure, and then toluene was added to the resulting residue, the obtained suspension filtered, and the resulting filtrate evaporated under reduced pressure to yield **18** as a yellow solid. ^1H NMR (C_6D_6, 300 MHz, 294 K): δ 7.10 (6H, d, J = 6 Hz, *o-H* aromatic), 6.90−6.75 (12H, m, aromatic), 6.55 (6H, d, J = 6 Hz, *m-H* aromatic), 3.26 (6H, s, OCH_3), 1.49 (3H, s, CH_3). Anal. Calcd for $C_{48}H_{51}ClHfN_6O_6$: C, 56.25; H, 5.31; N, 8.20; Cl, 3.46. Found: C, 52.36; H, 4.17; N, 9.58; Cl, 8.24.

General Procedure for the Polymerization of Propylene (ref 18). In a glovebox a mixture of 10 mg of the appropriate precatalyst and the appropriate amount of the MAO (1:1000, 1:500, or 1:100 metal:Al ratio) in 6 mL of toluene was loaded into a stainless steel reactor. The reactor was connected to a high-vacuum line, and the catalytic mixture was allowed to stir for 5 min at room temperature. The reactor was then frozen in liquid nitrogen, and 30 mL of propylene was condensed into the reactor. The reactor was then warmed to room temperature and stirred for 3 h. After this time, the reactor was opened in a well-ventilated hood to exhaust any excess of propylene gas, and the reaction was quenched by adding a 10% HCl solution in methanol to the mixture. The resulting polymer was washed with methanol followed by water, aqueous NaOH (1 M), water, and acetone and dried in a vacuum oven at 65 °C. The resulting polymer was fractionalized with heptane in a Soxhlet apparatus.[32]

General Procedure for the Polymerization of Ethylene (ref 14f). Similar to the polymerization of propylene, 10 mg of the precatalyst and the appropriate amount of MAO (1:1000, 1:500, or 1:100 metal:Al ratio) in 6 mL of toluene were loaded into a stainless steel reactor in a glovebox. The catalytic mixture was stirred for 5 min at room temperature, and ethylene gas was introduced. The pressure of the reactor was maintained at 9.86 atm (10 bar) during the entire polymerization (0.5 h). After this time, the reactor was opened in a well-ventilated hood to exhaust any excess of ethylene, and the reaction was quenched by adding a 10% HCl solution in methanol to the mixture. The resulting polymer was washed with methanol, water, aqueous NaOH (1 M), water, and acetone and then dried in a vacuum oven at 65 °C.

ESR Studies of the Active Species. *Preliminary Experiments.* A Teflon J. Young valve-sealed NMR tube was charged with complex **15** (5 mg), 0.5 mL of deuterated toluene, and MAO (M:Al = 1:100) inside a glovebox. The mixture was shaken thoroughly, and the EPR experiment carried out immediately.

Preparation of Samples for the Experiments with Radical Trapping Reagent (ref 17b). Preparation of each sample was performed inside a glovebox. Samples were first prepared in glass vials and then transferred to NMR tubes.

First sample: A mixture of complex **15** (5 mg, 7.58×10^{-6} mol) and MAO (Ti:Al = 1:100) was dissolved in 0.5 mL of a 2 mg/mL solution of C_{60} in toluene. The mixture was shaken thoroughly, and ESR was measured immediately. This sample imitates the activation stage in which the complex of Ti(IV) transforms to the paramagnetic complex of Ti(III) with the concomitant formation of a methyl radical, which is trapped by C_{60}. The sample was then subjected to MALDI-TOF mass spectroscopy experiments.

Second sample: This imitates the final stage of the activation, initiated by propylene, in which the cationic complex of Ti(IV) is formed. This stage is predicated by the formation of dimers or oligomers from propylene via intermediate radicals, which are expected to be trapped by C_{60}.

For the preparation of the second sample, a mixture of complex **15** (5 mg, 7.58×10^{-6} mol) and MAO (Ti:Al = 1:100) was dissolved in 0.5 mL of toluene, and only after the completion of this reaction was 0.5 mL of a 2 mg/mL toluene solution of fullerene added. The NMR tube was connected to a vacuum line, frozen, and then evacuated, followed by backfilling with ethylene at atmospheric pressure. The reaction mixture was shaken well, and the ESR spectrum measured immediately. The sample was then subjected to MALDI-TOF mass spectroscopy experiments.

Third and fourth sample: The sample preparation and experiment were performed in a similar manner to that of the second sample above with 15 mg (2.27×10^{-5} mol) or 50 mg (7.58×10^{-5} mol) of complex **15**.

■ ASSOCIATED CONTENT

Ⓢ Supporting Information

The details of the dynamic NMR studies of complexes **13** and **14** and the calculation of thermodynamic parameters for complex **14**, ^{13}C NMR spectra of the heptane-insoluble and heptane-soluble polypropylenes obtained from complexes **15** and **16** and crystallographic data for ligands **6** and **7** and complexes **8**, **9**, **10**, and **14**. This material is available free of charge via the Internet at http://pubs.acs.org.

■ AUTHOR INFORMATION

Corresponding Author

*E-mail: chmoris@tx.technion.ac.il.

Notes

The authors declare no competing financial interest.

[§]Deceased on September 25, 2013.

■ ACKNOWLEDGMENTS

This research was supported by the USA-Israel Binational Science Foundation under Contract 2008283. B.T. is grateful for the support to the Center for Absorption in Science, Ministry of Immigrant Absorption, State of Israel.

■ REFERENCES

(1) (a) *Topics in Catalysis*; Marks, T. J.; Stevens, J. C., Eds.; Baltzer: Basel, Switzerland, 1999; Vol. *15*. (b) Kaminsky, W. Olefin Polymerization Catalyzed by Metallocenes. In *Advances in Catalysis*; Gates, B. C.; Knozinger, H., Eds.; Academic Press: San Diego, CA,

2002; Vol. *46*, p 89. (c) Halterman, R. L. In *Metallocenes: Synthesis Reactivity Applications*; Togni, A.; Halterman, R. L., Eds.; Wiley-VCH: Weinheim, 1998; pp 455−539. (d) *Metallocene-Catalyzed Polymers: Materials, Properties, Processing and Markets*; Benedikt, G. M.; Goodall, B. L., Eds.; Plastics Design Library: New York, 1998; pp 1−386. (e) Coates, G. W.; Waymouth, R. M. Homogeneous Ziegler-Natta Catalysis. In *Comprehensive Organometallic Chemistry II*; Abel, E. W.; Stone, F. G. A.; Wilkinson, G., Eds.; Pergamon Press: Oxford, 1995; Vol. *12*, pp 1193−1208. (f) *Metallocene-Based Polyolefins. Preparation, Properties and Techniques*; Scheirs, J.; Kaminsky, W., Eds.; Wiley: New York, 1999; Vols. *1*−*2*. (g) Nomura, K. In *New Developments in Catalysis Research*; Bevy, L. P., Ed.; NOVA Science Publishers: New York, 2005; pp 199−217. (h) Okuda, J.; Eberle, T. In *Metallocenes: Synthesis Reactivity Applications*; Togni, A.; Halterman, R. L., Eds.; Wiley-VCH: Weinheim, 1998; pp 415−453.

(2) (a) Alt, H. G.; Koppl, A. *Chem. Rev.* **2000**, *100*, 1205−1222. (b) Coates, G. W. *Chem. Rev.* **2000**, *100*, 1223−1252. (c) Bryliakov, K. P.; Talsi, E. P. *Coord. Chem. Rev.* **2012**, *256*, 2994−3007. (d) Qian, Y.; Huang, J.; Bala, M. D.; Lian, B.; Zhang, H.; Zhang, H. *Chem. Rev.* **2003**, *103*, 2633−2690. (e) Gibson, V. C.; Spitzmesser, S. K. *Chem. Rev.* **2003**, *103*, 283−315. (f) McKnight, A. L.; Waymouth, R. M. *Chem. Rev.* **1998**, *98*, 2587−2598. (g) Halterman, R. L. *Chem. Rev.* **1992**, *92*, 965−994. (h) Fink, G.; Steinmetz, B.; Zechlin, J.; Przybyla, C.; Tesche, B. *Chem. Rev.* **2000**, *100*, 1377−1390. (i) Resconi, L.; Cavallo, L.; Fait, A.; Piemontesi, F. *Chem. Rev.* **2000**, *100*, 1253−1346. (j) Metallocene Complexes as Catalysts for Olefin Polymerization (special issue). Alt, H. G., Ed. *Coord. Chem. Rev.* **2006**, *250*, (1−2). (k) Ittel, S. D.; Johnson, L. K.; Brookhart, M. *Chem. Rev.* **2000**, *100*, 1169−1203. (l) Fujisawa, K.; Nabika, M. *Coord. Chem. Rev.* **2013**, *257*, 119−129. (m) Chen, E. Y.-X.; Marks, T. J. *Chem. Rev.* **2000**, *100*, 1391−1434. (n) Nomura, K.; Zhang, S. *Chem. Rev.* **2011**, *111*, 2342−2362. (o) Delferro, M.; Marks, T. J. *Chem. Rev.* **2011**, *111*, 2450−2485. (p) Valente, A.; Mortreux, A.; Visseaux, M.; Zinck, P. *Chem. Rev.* **2013**, *113*, 3836−3857.

(3) (a) Suhm, J.; Heinemann, J.; Worner, C.; Muller, P.; Stricker, F.; Kressler, J.; Okuda, J.; Mulhaupt, R. *Macromol. Symp.* **1998**, *129*, 1−28. (b) Metal-Catalysed Polymerisation (special issue). Milani, B.; Claver, C., Eds. *Dalton Trans.* **2009**, *41*, 8769−9076.

(4) (a) Sinn, H.; Kaminsky, W.; Vollmer, H. J.; Woldt, R. *Angew. Chem., Int. Ed. Engl.* **1980**, *19*, 390−392. (b) Kaminsky, W. *J. Chem. Soc., Dalton Trans.* **1998**, 1413−1418. (c) Kaminsky, W. *Macromol. Chem. Phys.* **1996**, *197*, 3907−3945. (d) Kaminsky, W.; Arndt, M. *Adv. Polym. Sci.* **1997**, *127*, 143−187. (e) Kaminsky, W.; Kulper, K.; Brintzinger, H. H.; Wild, F. R.W. P. *Angew. Chem., Int. Ed. Engl.* **1985**, *24*, 507−508. (f) Kaminsky, W. *J. Polym. Sci. A: Polym. Chem.* **2004**, *42*, 3911−3921. (g) Kaminsky, W.; Funck, A.; Hahnsen, H. *Dalton Trans.* **2009**, 8803−8810.

(5) (a) Ewen, J. A. *J. Am. Chem. Soc.* **1984**, *106*, 6355−6364. (b) Ewen, J. A.; Elder, M. J.; Jones, R. L.; Haspeslagh, L.; Atwood, J. L.; Bott, S. G.; Robinson, K. *Makromol. Chem., Macromol. Symp.* **1991**, *48/49*, 253−295.

(6) (a) Roberts, J. A. S.; Chen, M.-C.; Seyam, A. M.; Li, L.; Zuccaccia, C.; Stahl, N. G.; Marks, T. J. *J. Am. Chem. Soc.* **2007**, *129*, 12713−12733. (b) Luo, L.; Marks, T. J. *Top. Catal.* **1999**, *7*, 97−106. (c) Giardello, M. A.; Eisen, M. S.; Stern, C. L.; Marks, T. J. *J. Am. Chem. Soc.* **1995**, *117*, 12114−12129.

(7) (a) Cardin, D. J.; Lappert, M. F.; Raston, C. L. *Chemistry of Organo-Zirconium and -Hafnium Compounds*; Wiley: New York, 1986; pp 1−285. (b) Mashima, K.; Nakayama, Y.; Nakamura, A. *Adv. Polym. Sci.* **1997**, *133*, 1−51. (c) Bochmann, M. *J. Chem. Soc., Dalton Trans.* **1996**, 255−270. (d) Hamielec, A. E.; Soares, J. B. P. *Prog. Polym. Sci.* **1996**, *21*, 651−706. (e) Schobel, A.; Lanzinger, D.; Rieger, B. *Organometallics* **2013**, *32*, 427−437. (f) Xu, G.; Chung, T. C. *J. Am. Chem. Soc.* **1999**, *121*, 6763−6764. (g) Carpentier, J.-F.; Wu, Z.; Lee, C. W.; Stromberg, S.; Christopher, J. N.; Jordan, R. F. *J. Am. Chem. Soc.* **2000**, *122*, 7750−7767. (h) Brintzinger, H. H.; Fischer, D.; Muelhaupt, R.; Waymouth, R. M. *Angew. Chem., Int. Ed. Engl.* **1995**, *34*, 1143−1170. (i) Lancaster, S. J.; Bochmann, M. *Organometallics* **2001**, *20*, 2093−2101.

(8) (a) Sita, L. R.; Babcock, J. R. *Organometallics* **1998**, *17*, 5228−5230. (b) Zhang, Y.; Sita, L. R. *Chem. Commun.* **2003**, 2358−2359. (c) Epshteyn, A.; Trunkely, E. F.; Kissounko, D. A.; Fettinger, J. C.; Sita, L. R. *Organometallics* **2009**, *28*, 2520−2526. (d) Harney, M. B.; Keaton, R. J.; Fettinger, J. C.; Sita, L. R. *J. Am. Chem. Soc.* **2006**, *128*, 3420−3432. (e) Wei, J.; Hwang, W.; Zhang, W.; Sita, L. R. *J. Am. Chem. Soc.* **2013**, *135*, 2132−2135. (f) Sita, L. R. *Angew. Chem., Int. Ed.* **2011**, *50*, 6963−6965. (g) Keaton, R. J.; Sita, L. R. *J. Am. Chem. Soc.* **2002**, *124*, 9070−9071. (h) Jayaratne, K. C.; Sita, L. R. *J. Am. Chem. Soc.* **2000**, *122*, 958−959. (i) Zhang, Y.; Reeder, E. K.; Keaton, R. J.; Sita, L. R. *Organometallics* **2004**, *23*, 3512−3520. (j) Keaton, R. J.; Jayaratne, K. C.; Fettinger, J. C.; Sita, L. R. *J. Am. Chem. Soc.* **2000**, *122*, 12909−12910.

(9) (a) Kissounko, D. A.; Zabalov, M. V.; Brusova, G. P.; Lemenovskii, D. A. *Russ. Chem. Rev.* **2006**, *75*, 351−374. (b) Britovsek, G. J. P.; Gibson, V. C.; Wass, D. F. *Angew. Chem., Int. Ed.* **1999**, *38*, 428−447.

(10) (a) Tao, X.; Gao, W.; Huo, H.; Mu, Y. *Organometallics* **2013**, *32*, 1287−1294. (b) Stephan, D. W. *Organometallics* **2005**, *24*, 2548−2560. (c) Jian, Z.; Petrov, A. R.; Hangaly, N. K.; Li, S.; Rong, W.; Mou, Z.; Rufanov, K. A.; Harms, K.; Sundermeyer, J.; Cui, D. *Organometallics* **2012**, *31*, 4267−4282. (d) Littke, A.; Sleiman, N.; Bensimon, C.; Richeson, D. S.; Yap, G. P. A.; Brown, S. J. *Organometallics* **1998**, *17*, 446−451. (e) Xu, T.; Mu, Y.; Gao, W.; Ni, J.; Ye, L.; Tao, Y. *J. Am. Chem. Soc.* **2007**, *129*, 2236−2237.

(11) (a) Shi, X.-C.; Jin, G.-X. *Dalton Trans.* **2011**, *40*, 11914−11919. (b) Wang, L.; Wu, Q.; Xu, H.; Mu, Y. *Dalton Trans.* **2012**, *41*, 7350−7357. (c) Nomura, K.; Fukuda, H.; Katao, S.; Fujiki, M.; Kim, H. J.; Kim, D.-H.; Zhang, S. *Dalton Trans.* **2011**, *40*, 7842−7849. (d) Erben, M.; Merna, J.; Hylsky, O.; Kredatusova, J.; Lycka, A.; Padelkova, L.; Dostal, Z.; Novotny, M. *J. Organomet. Chem.* **2013**, *725*, 5−10. (e) Cano, J.; Kunz, K. *J. Organomet. Chem.* **2007**, *692*, 4411−4423. (f) Nomura, K.; Liu, J. Y.; Padmanabhan, S.; Kitiyanan, B. *J. Mol. Catal. A* **2007**, *267*, 1−29. (g) Nomura, K. *Dalton Trans.* **2009**, *38*, 8811−8823. (h) Tang, X. Y.; Wang, Y. X.; Liu, S. R.; Liu, J. Y.; Li, Y. S. *Dalton Trans.* **2013**, *42*, 499−506.

(12) (a) Makio, H.; Fujita, T. *Acc. Chem. Res.* **2009**, *42*, 1532−1544. (b) Connor, E. F.; Younkin, T. R.; Henderson, J. I.; Hwang, S.; Grubbs, R. H.; Roberts, W. P.; Litzau, J. J. *J. Polym. Sci., Part A: Polym. Chem.* **2002**, *40*, 2842−2854. (c) Younkin, T. R.; Connor, E. F.; Henderson, J. I.; Friedrich, S. K.; Grubbs, R. H.; Bansleben, D. A. *Science* **2000**, *287*, 460−462. (d) Wang, C.; Friedrich, S. K.; Younkin, T. R.; Li, R. T.; Grubbs, R. H.; Bansleben, D. A.; Day, M. W. *Organometallics* **1998**, *17*, 3149−3151. (e) Johnson, L. K.; Bennett, A. M. A.; Ittel, S. D.; Wang, L.; Parthasarathy, A.; Hauptman, E.; Simpson, R. D.; Feldman, J.; Coughlin, E. B. Patent WO 98/30609, 1998. (f) Keim, W.; Kowaldt, F. H.; Goddard, R.; Kruger, C. *Angew. Chem., Int. Ed. Engl.* **1978**, *17*, 466−467. (g) Starzewski, K. A. O.; Witte, J. *Angew. Chem., Int. Ed. Engl.* **1985**, *24*, 599−601. (h) Klabunde, U.; Ittel, S. D. *J. Mol. Catal.* **1987**, *41*, 123−134. (i) Klabunde, U.; Mulhaupt, R.; Herskovitz, T.; Janowicz, A. H.; Calabrese, J.; Ittel, S. D. *J. Polym. Sci., Polym. Chem.* **1987**, *25*, 1989−2003. (j) Johnson, L. K.; Killian, C. M.; Brookhart, M. *J. Am. Chem. Soc.* **1995**, *117*, 6414−6415. (k) Small, B. L.; Brookhart, M.; Bennett, A. M. A. *J. Am. Chem. Soc.* **1998**, *120*, 4049−4050. (l) Britovsek, G. J. P.; Gibson, V. C.; Kimberleyqq, B. S.; Maddox, P. J.; McTavish, S. J.; Solan, G. A.; White, A. J. P.; Williams, D. J. *Chem. Commun.* **1998**, 849−850. (m) Coates, G. W.; Hustad, P. D.; Reinartz, S. *Angew. Chem., Int. Ed.* **2002**, *41*, 2237−2257. (n) Camacho, D. H.; Salo, E. V.; Ziller, J. W.; Guan, Z. *Angew. Chem., Int. Ed.* **2004**, *43*, 1821−1825. (o) Atienza, C. C. H.; Milsmann, C.; Lobkovsky, E.; Chirik, P. J. *Angew. Chem., Int. Ed.* **2011**, *50*, 8143−8147. (p) Press, K.; Cohen, A.; Goldberg, I.; Venditto, V.; Mazzeo, M.; Kol, M. *Angew. Chem., Int. Ed.* **2011**, *50*, 3529−3532. (q) Li, L.; Metz, M. V.; Li, H.; Chen, M.-C.; Marks, T. J.; Liable-Sands, L.; Rheingold, A. L. *J. Am. Chem. Soc.* **2002**, *124*, 12725−12741. (r) Edson, J. B.; Wang, Z.; Kramer, E. J.; Coates, G. W. *J. Am. Chem. Soc.* **2008**, *130*, 4968−4977. (s) Matsui, S.; Mitani, M.; Saito, J.; Tohi, Y.; Makio, H.; Matsukawa, N.; Takagi, Y.; Tsuru, K.; Nitabaru, M.; Nakano, T.; Tanaka, H.; Kashiwa, N.; Fujita, T. *J. Am. Chem. Soc.*

2001, *123*, 6847−6856. (t) Igarashi, A.; Zhang, S.; Nomura, K. *Organometallics* **2012**, *31*, 3575−3581. (u) Li, G.; Lamberti, M.; Roviello, G.; Pellecchia, C. *Organometallics* **2012**, *31*, 6772−6778. (v) Shi, X.-C.; Jin, G.-X. *Organometallics* **2012**, *31*, 7198−7205. (w) Chuchuryukin, A. V.; Huang, R.; van Faassen, E. E.; van Klink, G. P. M.; Lutz, M.; Chadwick, J. C.; Spek, A. L.; van Koten, G. *Dalton Trans.* **2011**, *40*, 8887−8895. (x) Hou, X.; Liang, T.; Sun, W.-H.; Redshaw, C.; Chen, X. *J. Organomet. Chem.* **2012**, *708*−*709*, 98−105. (y) McGowan, K. P.; Veige, A. S. *J. Organomet. Chem.* **2012**, *711*, 10−14. (z) Suzuki, N.; Kobayashi, G.; Hasegawa, T.; Masuyama, Y. *J. Organomet. Chem.* **2012**, *717*, 23−28. (aa) Mehdiabadi, S.; Soares, J. B. P. *Macromolecules* **2013**, *46*, 1312−1324. (bb) Hagen, H.; Boersma, J.; van Koten, G. *Chem. Soc. Rev.* **2002**, *31*, 357−364. (cc) Gambarotta, S. *Coord. Chem. Rev.* **2003**, *237*, 229−243. (dd) Redshaw, C. *Dalton Trans.* **2010**, *39*, 5595−5604.

(13) (a) Edelmann, F. T. *Chem. Soc. Rev.* **2009**, *38*, 2253−2268. (b) Collins, S. *Coord. Chem. Rev.* **2011**, *255*, 118−138. (c) Edelmann, F. T. *Chem. Soc. Rev.* **2012**, *41*, 7657−7672. (d) Edelmann, F. T. *Adv. Organomet. Chem.* **2008**, *57*, 183−352.

(14) (a) Volkis, V.; Shmulinson, M.; Averbuj, C.; Lisovskii, A.; Edelmann, F. T.; Eisen, M. S. *Organometallics* **1998**, *17*, 3155−3157. (b) Volkis, V.; Nelkenbaum, E.; Lisovskii, A.; Hasson, G.; Semiat, R.; Kapon, M.; Botoshansky, M.; Eishen, Y.; Eisen, M. S. *J. Am. Chem. Soc.* **2003**, *125*, 2179−2194. (c) Nelkenbaum, E.; Kapon, M.; Eisen, M. S. *Organometallics* **2005**, *24*, 2645−2659. (d) Smolensky, E.; Eisen, M. S. *Dalton Trans.* **2007**, 5623−5650. (e) Richter, J.; Edelmann, F. T.; Noltemeyer, M.; Schmidt, H. G.; Shmulinson, M.; Eisen, M. S. *J. Mol. Catal. A: Chem.* **1998**, *130*, 149−162. (f) Herskovics-Korine, D.; Eisen, M. S. *J. Organomet. Chem.* **1995**, *503*, 307−314. (g) Domeshek, E.; Batrice, R. J.; Aharonovich, S.; Tumanskii, B.; Botoshansky, M.; Eisen, M. S. *Dalton Trans.* **2013**, *42*, 9069−78. (h) Volkis, V.; Shmulinson, M.; Shaviv, E.; Lisovskii, A.; Plat, D.; Kuhl, O.; Koch, T.; Hey-Hawkins, E.; Eisen, M. S. *PMSEP reprints*, 223rd ACS National Meeting, Orlando, FL, April 7−11, 2002; American Chemical Society: Washington, DC, 2002; Vol. *86*, pp 301−303. (i) Averbuj, C.; Tish, E.; Eisen, M. S. *J. Am. Chem. Soc.* **1998**, *120*, 8640−8646.

(15) (a) Walther, D.; Fischer, R.; Gorls, H.; Koch, J.; Schweder, B. *J. Organomet. Chem.* **1996**, *508*, 13−22. (b) Hagadorn, J. R.; Arnold, J. *J. Chem. Soc., Dalton Trans.* **1997**, 3087−3096. (c) Flores, J. C.; Chien, J. C. W.; Rausch, M. D. *Organometallics* **1995**, *14*, 1827−1833. (d) Coles, M. P.; Jordan, R. F. *J. Am. Chem. Soc.* **1997**, *119*, 8125−8126. (e) Takeuchi, D. *Dalton Trans.* **2010**, *39*, 311−328. (f) Kirillov, E.; Roisnel, T.; Carpentier, J. F. *Organometallics* **2012**, *31*, 3228−3240. (g) Otten, E.; Dijkstra, P.; Visser, C.; Meetsma, A.; Hessen, B. *Organometallics* **2005**, *24*, 4374−4386. (h) Sciarone, T. J. J.; Nijhuis, C. A.; Meetsma, A.; Hessen, B. *Dalton Trans.* **2006**, 4896−4904. (i) Bai, S.-D.; Guan, F.; Hu, M.; Yuan, S.-F.; Guo, J.-P.; Liu, D.-S. *Dalton Trans.* **2011**, *40*, 7686−7688. (j) Busico, V.; Cipullo, R.; Caporaso, L.; Angelini, G.; Segre, A. L. *J. Mol. Catal. A: Chem.* **1998**, *128*, 53−64.

(16) (a) Keaton, R. J.; Jayaratne, K. C.; Henningsen, D. A.; Koterwas, L. A.; Sita, L. R. *J. Am. Chem. Soc.* **2001**, *123*, 6197−6198. (b) Gomez, R.; Duchateau, R.; Chernega, A. N.; Teuben, J. N.; Edelmann, F. T.; Green, M. L. H. *J. Organomet. Chem.* **1995**, *491*, 153−158. (c) Hagadorn, J. R.; Arnold, J. *Organometallics* **1998**, *17*, 1355−1368. (d) Hagadorn, J. R.; Arnold, J. *J. Am. Chem. Soc.* **1996**, *118*, 893−894. (e) Edelmann, F. T. *Coord. Chem. Rev.* **1994**, *137*, 403−481. (f) Edelmann, F. T. *Top. Curr. Chem.* **1996**, *179*, 113−148. (g) Hagadorn, J. R.; Arnold, J. *Organometallics* **1994**, *13*, 4670−4672. (h) Roesky, P. W. *Z. Anorg. Allg. Chem.* **2003**, *629*, 1881−1894. (i) Edelmann, F. T. *Struct. Bonding (Berlin)* **2010**, *137*, 109−163.

(17) (a) Volkis, V.; Lisovskii, A.; Tumanskii, B.; Shuster, M.; Eisen, M. S. *Organometallics* **2006**, *25*, 2656−2666. (b) Volkis, V.; Tumanskii, B.; Eisen, M. S. *Organometallics* **2006**, *25*, 2722−2724. (c) Aharonovich, S.; Volkis, V.; Eisen, M. S. *Macromol. Symp.* **2007**, *260*, 165−171. (d) Volkis, V.; Aharonovich, S.; Eisen, M. S. *Macromol. Res.* **2010**, *18*, 967−973. (e) Volkis, V.; Rodensky, M.; Lisovskii, A.; Balazs, Y.; Eisen, M. S. *Organometallics* **2006**, *25*, 4934−4937.

(18) (a) Aharonovich, S.; Botoshansky, M.; Balazs, Y. S.; Eisen, M. S. *Organometallics* **2012**, *31*, 3435−3438. (b) Aharonovich, S. *Heteroazaallyl Complexes of Li, Ti, Zr, and V: Structure, Reactivity and Catalytic Propylene Polymerization*. Ph.D. Thesis, Technion-Israel Institute of Technology, 2010.

(19) Elkin, T.; Aharonovich, S.; Botoshansky, M.; Eisen, M. S. *Organometallics* **2012**, *31*, 7404−7414.

(20) Taylor, E. C.; Ehrhart, W. A. *J. Org. Chem.* **1963**, *28*, 1108−1112.

(21) Kosturkiewicz, Z.; Ciszak, E.; Tykarska, E. *Acta Crystallogr.* **1992**, *B48*, 471−476.

(22) (a) Jeffrey, G. A.; Saenger, W. *Hydrogen Bonding in Biological Structures*; Springer: Berlin, 1991; pp 147−155. (b) Gavrani, M.; Kaitner, B.; Metrovi, E. *J. Chem. Crystallogr.* **1996**, *26*, 23−28. (c) Etter, M. C. *J. Phys. Chem.* **1991**, *95*, 4601−4610. (d) Grabowski, S. J. *Hydrogen Bonding-New Insights*; Springer, 2006; pp 1−519.

(23) (a) Rofouei, M. K.; Sohrabi, N.; Shamsipur, M.; Fereyduni, E.; Ayyappan, S.; Sundaraganesan, N. *Spectrochim. Acta Part A* **2010**, *76*, 182−190. (b) Yeh, C.-W.; Hu, H.-L.; Liang, R.-H.; Wang, K.-M.; Yen, T.-Y.; Chen, J.-D.; Wang, J.-C. *Polyhedron* **2005**, *24*, 539−548. (c) Ren, T.; Radak, S.; Ni, Y.; Xu, G.; Lin, C.; Shaffer, K. L.; DeSilva, V. *J. Chem. Crystallogr.* **2002**, *32*, 197−203.

(24) Hafelinger, G.; Kuske, K. H. In *The Chemistry of the Amidines and Imidates*; Patai, S.; Rappoport, Z., Eds.; Wiley: Chichester, 1991; Vol. *2*, pp 1−100.

(25) (a) Meschede, L.; Limbach, H.-H. *J. Phys. Chem.* **1991**, *95*, 10267−10280. (b) Komber, H.; Limbach, H.-H.; Bohme, F.; Kunert, C. *J. Am. Chem. Soc.* **2002**, *124*, 11955−11963. (c) Darowska, M.; Rudka, T.; Raczynska, E. D. *Chem. Pap.* **2003**, *57*, 216−223. (d) Anulewicz, R.; Wawer, I.; Krygowski, T. M.; Mannle, F.; Limbach, H.-H. *J. Am. Chem. Soc.* **1997**, *119*, 12223−12230.

(26) Kuhn, K. M.; Grubbs, R. H. *Org. Lett.* **2008**, *10*, 2075−2077.

(27) (a) Glockner, A.; Tamm, M. *Chem. Soc. Rev.* **2013**, *42*, 128−142. (b) Therrien, B.; Konig, A.; Ward, T. R. *Organometallics* **1999**, *18*, 1565−1568. (c) Mthiruaine, C. M.; Friedrich, H. B.; Changamu, E. O.; Fernandes, M. A. *Acta Crystallogr.* **2012**, *E68*, m931.

(28) Data from CCDC: http://www.ccdc.cam.ac.uk/Solutions/CSDSystem/Pages/CSD.aspx.

(29) Bai, S.-D.; Tong, H.-B.; Guo, J.-P.; Zhou, M.-S.; Liu, D.-S. *Inorg. Chim. Acta* **2009**, *362*, 1143−1148.

(30) Sun, J.-F.; Chen, S.-J.; Duan, Y.; Li, Y.-Z.; Chen, X.-T.; Xue, Z.-L. *Organometallics* **2009**, *28*, 3088−3092.

(31) (a) Boere, R. T.; Klassen, V.; Wolmershauser, G. *J. Chem. Soc., Dalton Trans.* **1998**, 4147−4154. (b) Gomez-Suarez, A.; Ramon, R. S.; Songis, O.; Slawin, A. M. Z.; Cazin, C. S. J.; Nolan, S. P. *Organometallics* **2011**, *30*, 5463−5470.

(32) Pasquin, I. *Pure Appl. Chem.* **1967**, *15*, 465−480.

(33) (a) Hamielec, A. E.; Soares, J. B. P. *Prog. Polym. Sci.* **1996**, *21*, 651−706. (b) Liguori, D.; Centore, R.; Tuzi, A.; Grisi, F.; Sessa, I.; Zimbelli, A. *Macromolecules* **2003**, *36*, 5451−5458. (c) Eguchi, K.; Machida, M.; Yamanaka, I. *Science and Technology in Catalysis 2006*: Proceedings of the Fifth Tokyo Conference on Advanced Catalytic Science and Technology, Tokyo, July 23−28, 2006; pp 1−631.

(34) (a) Flisak, Z.; Ziegler, T. *Proc. Natl. Acad. Sci. U.S.A.* **2006**, *103*, 15338−15342. (b) Bochmann, M. *Organometallics* **2010**, *29*, 4711−4740. (c) Bochmann, M. *Acc. Chem. Res.* **2010**, *43*, 1267−1278.

(35) (a) Krusic, P. J.; Wasserman, E.; Keizer, P. N.; Morton, J. R.; Preston, K. F. *Science* **1991**, *254*, 1183−1185. (b) Tumanskii, B. L.; Kalina, O. G. *Radical Reactions of Fullerenes and Their Derivatives: Developments in Fullerene Studies-2*; Kluwer Academic Publishers: Dodrecht, The Netherlands, 2001; pp 62−63.

(36) (a) Bryliakov, K. P.; Semikolenova, N. V.; Zakharov, V. A.; Talsi, E. P. *J. Organomet. Chem.* **2003**, *683*, 23−28. (b) Sharma, M.; Yameen, H. S.; Tumanskii, B.; Filimon, S.-A.; Tamm, M.; Eisen, M. S. *J. Am. Chem. Soc.* **2012**, *134*, 17234−17244.

(37) *Kappa CCD Server Software*; Nonius BV: Delft, The Netherlands, 1997.

(38) Otwinowski, Z.; Minor, W. *Methods Enzymol.* **1997**, *276*, 307−326.

(39) Sheldrick, G. M. *Acta Crystallogr., Sect. A* **1990**, *A46*, 467−473.

(40) *ORTEP*, TEXSAN Structure Analysis Package; Molecular Structure Corp.: The Woodlands, TX, 1999.
(41) Mercury Software from CCDC: http://www.ccdc.cam.ac.uk/Solutions/CSDSystem/Pages/Mercury.aspx.
(42) Manxzer, L. E.; Deaton, J.; Sharp, P.; Schrock, R. R. *Inorg. Synth.* **1982**, *21*, 135−140.
(43) Bradey, D. C.; Thomas, I. M. *J. Chem. Soc.* **1960**, 3857−3861.
(44) Binobaid, A.; Iglesias, M.; Beetstra, D. J.; Kariuki, B.; Dervisi, A.; Fallis, I. A.; Cavell, K. J. *Dalton Trans.* **2009**, 7099−7112.